
Response to the First Referee

Reviewer #1:

This paper by Yan et al. investigated the characteristics of winter haze episodes in Jingzhou of Central China under typical potential synoptic controls (PSCs) during November 2013-February 2014. Furthermore, they examined the contributions of local and transport of pollutants from surrounding regions to PM_{2.5} under different PSCs by applying the GEOS-Chem model with a high resolution. This work also studied the effectiveness of different emission control strategies in Jingzhou, Central China, and other surrounding regions under different PSCs, and highlights the importance of collaborative actions for PM_{2.5} mitigation under server haze pollution. In general, the study is well organized and worthy of publication. However, I have some specific comments that I feel deserve attention.

We thank the reviewer for comments, which have been incorporated to improve the manuscript.

Major comments

1. The writing should be improved before publication.

We thank the referee for this comment. We have made necessary corrections to grammar throughout the text (see details in the revision manuscript). We have polished the manuscript for all the authors.

2. The configuration of the model is vague. How many nested domains were applied in each simulation? What is the geographic coverage of each domain and the corresponding resolution? What are the emission inventories for each domain? A figure showing each nested domain is also highly recommended.

We thank the referee for this comment. We have added a figure in the revised file of supporting information to explain the geographic coverage of each domain and the corresponding resolution for GEOS_Chem global model ($2^\circ \times 2.5^\circ$, providing boundary condition to nested model) and nested model ($70^\circ\text{E}-140^\circ\text{E}$, $15^\circ\text{S}-55^\circ\text{N}$; $0.25^\circ \times 0.3125^\circ$). The emission inventories for each domain are shown in the revised Table S1 and Table S2. We also revised the description in the text of Sect. 2.3.

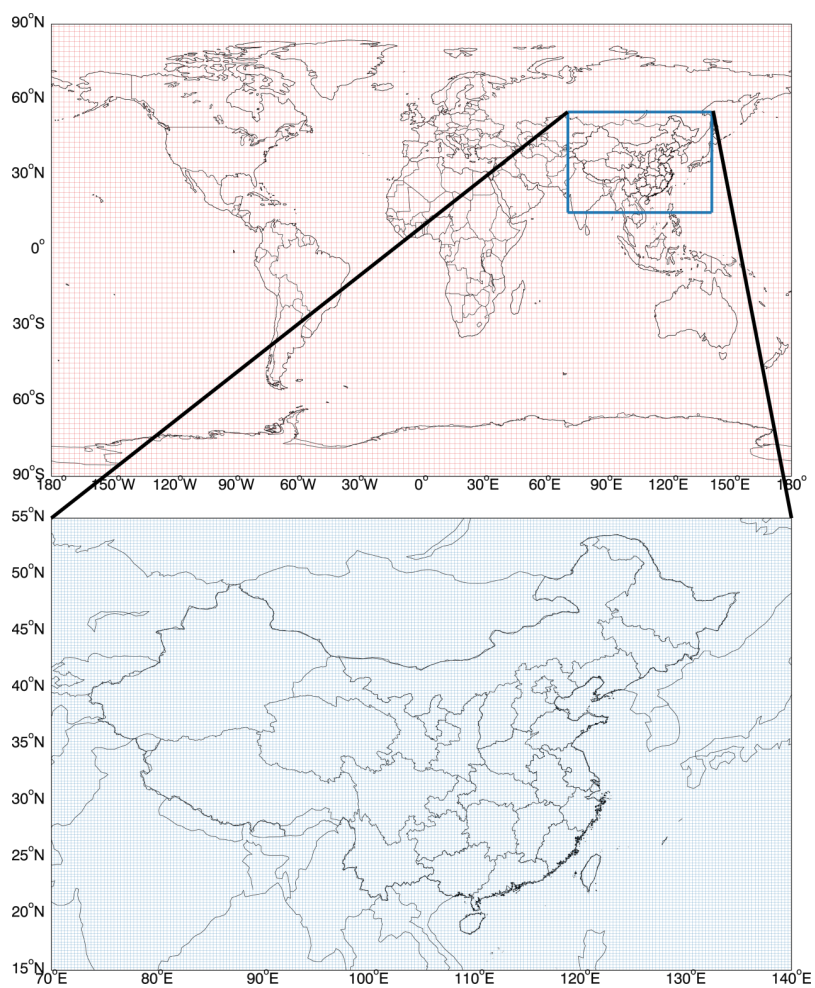


Figure S3 The geographic coverage of each domain and the corresponding resolution for GEOS_Chem global model ($2^{\circ} \times 2.5^{\circ}$) and nested model (70°E - 140°E , 15°S - 55°N ; $0.25^{\circ} \times 0.3125^{\circ}$).

[illegible]

Global	MEGAN	MEGAN v2.1 biogenic emissions	—	2013-2014	ISOP, monoterpenes, sesquiterpenes, MOH, ACET, ETOH, CH ₂ O, ALD ₂ , HCOOH, C ₂ H ₄ , TOLU, PRPE	Guenther et al. (2012)
Other natural emission inventory						
Global	SoilNOx	Emission of NO _x from soils and fertiliser use	—	2013-2014	NO	Hudman et al. (2012)
Global	LightNOx	NO _x from lightning	—	2013-2014	NO	Murray et al. (2012)

1. RETRO includes PRPE, ALK₄, ALD₂, CH₂O and MEK; in the CTM, MEK emissions are further allocated to MEK (25 %) and ACET (75 %). AEIC and MEIC include PRPE, C₂H₆, C₃H₈, ALK₄, ALD₂, CH₂O, MEK and ACET. NEI2011 includes PRPE, C₃H₈, ALK₄, CH₂O, MEK and ACET. EMEP includes PRPE, ALK₄, ALD₂ and MEK. Emissions of C₂H₆ outside Asia are from Xiao et al. (2008).

Table S2 Anthropogenic and natural source emission inventories adopted in the GEOS-Chem nested modelling of this study

Region	Abbreviation	Description	Resolution	Year	Species	Reference
Anthropogenic emission inventory						
Non-China	EDGAR	EDGAR v4.2 anthropogenic + biofuel	0.1°×0.1°, monthly	2013-2014	NO _x , SO ₂ , SO ₄ ²⁻ , CO, NH ₃	http://edgar.jrc.ec.europa.eu/overview.php?v=42
Nested domain	BOND	BOND biofuel + anthropogenic BC + OC emissions	1°×1°, monthly	2000	BC and OC	Bond et al. (2007)
Non-China	RETRO	RETRO anthropogenic + biofuel	0.5°×0.5°, monthly	2000	NMVOCs ¹ except C ₂ H ₆ and C ₃ H ₈	ftp://ftp.retro.enes.org/pub/emissions/aggregated/anthro/0.5x0.5/2000/
Nested domain	SHIP	ICOADS ship emissions	1°×1°, monthly	2002	NO _x , SO ₂ , CO	Wang et al. (2008)

Nested domain	AEIC	Aircraft emissions	1°×1°, monthly	2005	NO _x , SO ₂ , CO, NMVOCs ¹ , BC, OC	
China	MEIC	MEIC inventory for China	0.25°×0.25°, monthly	2013-2014	NO _x , SO ₂ , CO, NMVOCs ¹ , NH ₃	http://www.meicmodel.org/ .
Central China	SEEA	SEEA	0.1°×0.1°, monthly	2017	NO _x , SO ₂ , CO, NH ₃ , VOCs	
Biomass burning emission inventory						
Nested domain	GFED4	GFED4 biomass burning inventory	0.25°×0.25°, monthly	2013-2014	NO _x , SO ₂ , CO, NMVOCs, NH ₃ , BC, OC	http://www.globalfiredata.org , Giglio et al. (2013)
Biogenic emission inventory						
Nested domain	MEGAN	MEGAN v2.1 biogenic emissions	—	2013-2014	ISOP, monoterpenes, sesquiterpenes, MOH, ACET, ETOH, CH ₂ O, ALD ₂ , HCOOH, C ₂ H ₄ , TOLU, PRPE	Guenther et al. (2012)
Other natural emission inventory						
Nested domain	SoilNO _x	Emission of NO _x from soils and fertiliser use	—	2013-2014	NO	Hudman et al. (2012)
Nested domain	LightNO _x	NO _x from lightning	—	2013-2014	NO	Murray et al. (2012)

1. RETRO includes PRPE, ALK₄, ALD₂, CH₂O and MEK; in the CTM, MEK emissions are further allocated to MEK (25 %) and ACET (75 %). AEIC and MEIC include PRPE, C₂H₆, C₃H₈, ALK₄, ALD₂, CH₂O, MEK and ACET. NEI2011 includes PRPE, C₃H₈, ALK₄, CH₂O, MEK and ACET. EMEP includes PRPE, ALK₄, ALD₂ and MEK. Emissions of C₂H₆ outside Asia are from Xiao et al. (2008)

3. The circulation classification is the basis of all the analysis. Why did you choose the Lamb-Jenkenson method? What are the advantages of this method compared to the ones used in other studies such as Chang and Zhan, 2017, Dai et al., 2021, etc.?

We thank the referee for this comment. We have reviewed the advantages of Lamb-Jenkenson method with respect to the ones used in other studies in the revised Sect. 2.2: “Compared to the objective classification method PCA used in some studies (Chang and Zhan, 2017, Dai et al., 2021), this Lamb-Jenkenson method is a combination of subjective and objective methods. After the objective judgment of the circulation, we also make subjective considerations to overcome the weaknesses of their respective, leading to better synoptic significance. Many works of circulation classification have used the Lamb-Jenkenson method and reported that the analysis can well respond to the classification results (Philipp et al., 2016; Santurtun et al., 2015; Pope et al., 2015; Russo et al., 2014; Trigo et al., 2014; Trigo and DaCamara, 2000).”

Philipp, A., Beck, C., Huth, R., and Jacobeit, J.: Development and comparison of circulation type classifications using the COST 733 dataset and software, *International Journal of Climatology*, 36, 2673-2691, 10.1002/joc.3920, 2016.

Pope, R. J., Savage, N. H., Chipperfield, M. P., Arnold, S. R., and Osborn, T. J.: The influence of synoptic weather regimes on UK air quality: analysis of satellite column NO₂, *Atmospheric Science Letters*, 15, 211-217, 10.1002/asl2.492, 2014.

Pope, R. J., Savage, N. H., Chipperfield, M. P., Ordonez, C., and Neal, L. S.: The influence of synoptic weather regimes on UK air quality: regional model studies of tropospheric column NO₂, *Atmospheric Chemistry and Physics*, 15, 11201-11215, 10.5194/acp-15-11201-2015, 2015.

Russo, A., Trigo, R. M., Martins, H., and Mendes, M. T.: NO₂, PM₁₀ and O₃ urban concentrations and its association with circulation weather types in Portugal, *Atmospheric Environment*, 89, 768-785, 10.1016/j.atmosenv.2014.02.010, 2014.

Santurtun, A., Carlos Gonzalez-Hidalgo, J., Sanchez-Lorenzo, A., and Teresa Zarrabeitia, M.: Surface ozone concentration trends and its relationship with weather types in Spain (2001-2010), *Atmospheric Environment*, 101, 10-22, 10.1016/j.atmosenv.2014.11.005, 2015.

Trigo, R. M., and DaCamara, C. C.: Circulation weather types and their influence on the precipitation regime in Portugal, *International Journal of Climatology*, 20, 1559-1581, 10.1002/1097-0088(20001115)20:13<1559::aid-joc555>3.0.co;2-5, 2000.

4. The validation of model performances is very weak. The bias of the modeled PM_{2.5} in Jingzhou can be as high as more than 100 µg/m³, what are the possible reasons? The authors simply claimed the uncertainties in emissions, meteorology, and chemistry might cause this discrepancy without any details. What are the amount of the PM_{2.5}

precursors emitted in this study and how are the values compared to the published literature? How about the meteorological parameters used by the model vs. observations? The authors claimed an improvement in sulfate by the increase in primarily emitted sulfate in the model, how is that compared with observations? They also analyzed the changes in the chemical composition of PM_{2.5} under different typical PSCs without examination of the model performances in the base case.

Thanks for this query and suggestion, which are valuable for us to improve this work.

In order to better evaluate the GEOS-Chem model performances, the spatial distribution of PM_{2.5} concentrations averaged over the four typical heavy pollution processes simulated by the control (CON) simulation are compared with the observations (a total of 633 sites) from Ministry of Ecology and Environment of China (<http://www.mee.gov.cn/>) (revised Fig. 6). Similar to the underestimation in PM_{2.5} at Jingzhou, the underestimation is on a national scale when compared with the MEE observations, with a bias of -29.3 $\mu\text{g}/\text{m}^3$, -18.7 $\mu\text{g}/\text{m}^3$, -39.0 $\mu\text{g}/\text{m}^3$ and -21.4 $\mu\text{g}/\text{m}^3$ on average for SW-type, NW-type, A-type and C-type synoptic pattern, respectively (Fig. 6).

In order to explain the causes of the model discrepancy, we have added Table S3 to show the observed (modeled) meteorological conditions averaged over these four pollution episodes controlled by SW-type, NW-type, A-type and C-type synoptic pattern, respectively. There is an overestimate in temperature and wind speed and an underestimation in humidity, which can partly contribute to the underestimation of modeled PM_{2.5} concentrations. In addition, anthropogenic emissions for PM_{2.5} precursors used here are for the year 2017 over Central China from our newly developed SEEA inventory (Table S4). From 2013 to 2017, anthropogenic NO_x, SO₂, and primary PM_{2.5} emissions in Central China have declined substantially (Table S4), due to the implementation of stringent emission control measures for the 12th-13th Five-Year Plans (Zheng et al., 2018). The anthropogenic emissions biases may affect our simulations and PM_{2.5} attribution results to some extent.

We have no observations of the chemical compositions of PM_{2.5}. In order to examine the model performances in the PM_{2.5} chemical compositions, we have added Table 4 to review the reported concentrations of PM_{2.5} and the three inorganic salts (sulfate, nitrate and ammonium) in other cities. The contributions of sulfate, nitrate and ammonium are 9.1%-31.9%, 5.7%-32.1% and 5.9%-13.3%, respectively. In the CON simulation, the fractions of each inorganic salt to PM_{2.5} for these four typical heavy pollution processes are shown in revised Fig. S10, which are comparable to the previous results (Table 4).

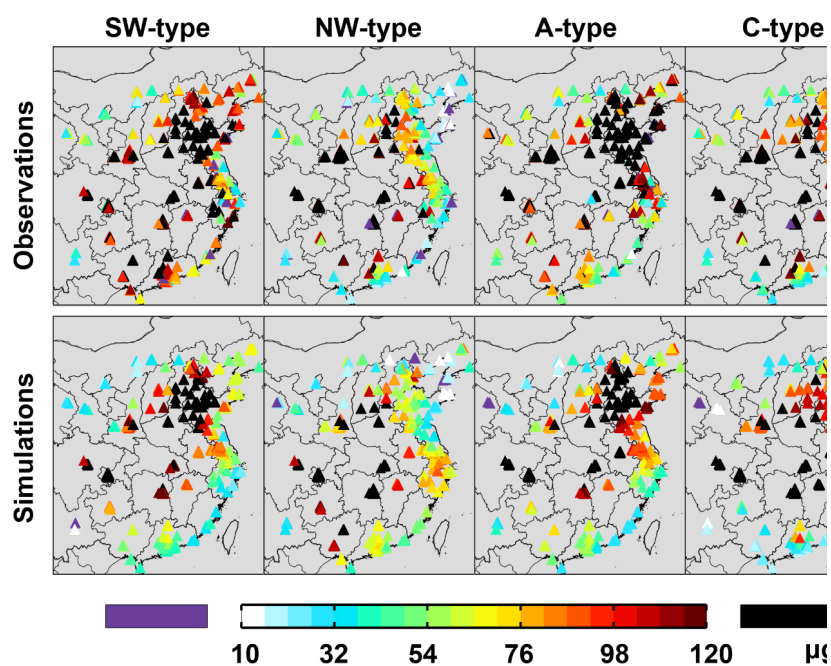


Figure 6 Spatial distribution of observed (top row) and modeled (bottom row, by CON case) $PM_{2.5}$ concentrations ($\mu g/m^3$) averaged over four severe pollution episodes controlled by SW-type (first column), NW-type (second column), A-type (third column) and C-type (fourth column) synoptic pattern, respectively.

Table S3. The observed (modeled) meteorological conditions at Jingzhou averaged over these four pollution episodes controlled by SW-type, NW-type, A-type and C-type synoptic pattern, respectively.

PSC	Temperature ($^{\circ}C$)	Humidity (%)	Pressure (kpa)	Wind speed (m/s)
SW	11.79 (12.96)	75.33 (69.25)	1018.33 (1024.06)	2.13 (3.09)
NW	3.61 (6.34)	71.16 (62.78)	1027.53 (1031.53)	1.44 (2.45)
A	5.81 (7.52)	64.96 (60.38)	1026.63 (1028.66)	1.45 (2.27)
C	9.60 (13.08)	78.10 (71.40)	1011.48 (1014.24)	1.88 (3.11)

Table S4. The emission amount of $PM_{2.5}$ precursors over Central China calculated from

85 SEEA (for the year 2017) and MEIC (for the years of 2013, 2014 and 2017) inventory
86 (unit: 10⁴ ton).

Category	SO ₂	NO _x	NH ₃	PM _{2.5}	CO	BC	OC	VOCs
SEEA (2017)	48.4	94.0	54.6	26.4	553.8	6.2	12.9	117.2
MEIC (2017)	52.0	70.4	57.5	35.2	629.2	6.8	11.7	116.4
MEIC (2013)	173.3	98.4	62.4	54.5	836.5	9.2	16.7	116.6
MEIC (2014)	97.0	80.0	61.1	46.8	744.2	8.3	15.3	116.4

87

88 Table 4 The reported concentrations of PM_{2.5} and the three inorganic salts (sulfate,
89 nitrate and ammonium, µg/m³) in other cities.

References	Site	Time	PM _{2.5}	Sulfate	Nitrate	Ammonium
Cao et al., 2012	Beijing	01/03	115.6±46.6	20.0±4.2 (17.3%)	13.1±4.5 (11.3%)	9.4±4.1 (8.1%)
Cao et al., 2012	Qingdao	01/03	134.8±43.0	21.1±7.7 (15.7%)	19.3±9.2 (14.3%)	15.3±5.2 (11.4%)
Cao et al., 2012	Tianjin	01/03	203.1±76.2	32.5±15. 1	25.2±10. 3	22.2±9.8 (10.9%)
Cao et al., 2012	Xi'an	01/03	356.3±118. 4	53.8±25. 6	29.0±10. 0	29.8±11.5 (8.4%)
Cao et al., 2012	Chongqing	01/03	316.6±101. 2	60.9±19. 6	18.1±6.4 (5.7%)	28.8±8.9 (9.1%)
Cao et al., 2012	Hangzhou	01/03	177.3±59.5	33.4±16. 7	25.7±14. 8	19.1±10.7 (10.8%)

				21.6±12.		
Cao et al., 2012	Shanghai	01/03	139.4±50.6	3	17.5±8.7 (12.6%)	14.5±5.9 (10.4%)
				(15.5%)		
				31.4±15.	22.2±10.	
Cao et al., 2012	Wuhan	01/03	172.3±67.0	6	7	18.4±10.2 (10.7%)
				(18.2%)	(12.9%)	
Zhang et al., 2011	Xi'an	03/06-03/07	194.1	35.6 (18.3%)	16.4 (8.4%)	11.4 (5.9%)
				44.8±31.	20.5±14.	
Huang et al., 2012	Xi'an	01/06-02/06	235.8±125.	3	2	14.5±10.8 (6.1%)
			1	(19.0%)	(8.7%)	
				14.4±9.2	33.4±23.	
Wang et al., 2020	Jinan	10/17	104±54	(13.8%)	2	13.0±8.3 (12.5%)
				(32.1%)		
				19.3±19.	42.8±41.	
Wang et al., 2020	Shijiazhuang	10/17	152±109	6	1	18.2±17.1 (12.0%)
	g			(12.7%)	(28.2%)	
				13.6±3.2	26.6±11.	
Wang et al., 2020	Wuhan	12/17	117±33	(11.6%)	1	13.1±3.8 (11.2%)
				(22.7%)		
				48±36	31±19	21±16
Wang et al., 2016a	Zhengzhou	01/11-02/11	297±160	(16.2%)	(10.4%)	(7.1%)
				23±10	22±9	16±5
Wang et al., 2016a	Zhengzhou	01/12-02/12	234±125	(9.8%)	(9.4%)	(6.8%)
				56±39	39±20	31±18
Wang et al., 2016a	Zhengzhou	01/13-02/13	337±168	(16.6%)	(11.6%)	(9.2%)
				40.1±19.	18.1±9.0	21.7±10.2
Luo et al., 2018	Zibo	12/06-02/07	224.9±85.4	2	(8.1%)	(9.7%)

				(17.9%)		
Wang et al., 2016b	Shanghai	12/11, 12/12, 12/13	73.9±57.5	12.2±9.2 (16.5%)	14.6±12.2 (19.8%)	8.2±6.7 (11.1%)
Xu et al., 2019	Beijing	02/17-03/17	180.5	20.1 (11.1%)	45.6 (25.3%)	22.5 (12.5%)
Xu et al., 2019	Beijing	05/17-09/17	186.7	20.2 (10.8%)	32.4 (17.4%)	17.1 (9.2%)
Xu et al., 2019	Beijing	10/17-11/17	167.5	17.9 (10.7%)	44.5 (26.6%)	20.9 (12.5%)
Zheng et al., 2016	Beijing	03/10-05/10	65.2±65.1	11.1±10.1 1 (17.0%)	11.1±11.0 0 (17.0%)	6.8±6.7 (10.4%)
Zheng et al., 2016	Beijing	07/09-08/09	88.9±39.1	23.0±13.9 9 (25.9%)	16.2±11.6 8 (18.2%)	11.8±6.8 (13.3%)
Zheng et al., 2016	Beijing	12/09-02/10	84.0±66.6	8.1±8.3 (9.1%)	8.0±9.6 (9.0%)	5.9±7.1 (6.6%)
Zheng et al., 2016	Guangzhou	11/10	73.3±16.5	16.6±4.0 (22.6%)	5.7±3.8 (7.8%)	6.2±2.0 (8.5%)
Zheng et al., 2016	Shenzhen	12/09	64.6±24.7	20.6±3.5 (31.9%)	4.9±3.5 (7.6%)	4.6±1.0 (7.1%)
Zheng et al., 2016	Wuxi	04/10-05/10	82.1±27.0	12.8±3.8 (15.6%)	9.9±6.3 (12.1%)	7.0±2.0 (8.5%)
Zheng et al., 2016	Jinhua	10/11-11/11	81.9±26.2	18.3±6.7 (22.3%)	12.6±7.0 (15.4%)	10.4±4.1 (12.7%)
Liu et al., 2018	Chongqing	2012-2013	73.5±30.5	19.7±9.6 (26.8%)	6.5±6.2 (8.8%)	6.1±2.7 (8.3%)

Liu et al., 2018	Shanghai	2012-2013	68.4±20.3	13.6±6.4 (19.9%)	11.9±5.0 (17.4%)	5.8±2.1 (8.5%)
Liu et al., 2018	Beijing	2012-2013	71.7±36.0	11.9±8.2 (16.6%)	9.3±7.5 (13.0%)	5.3±2.7 (7.4%)

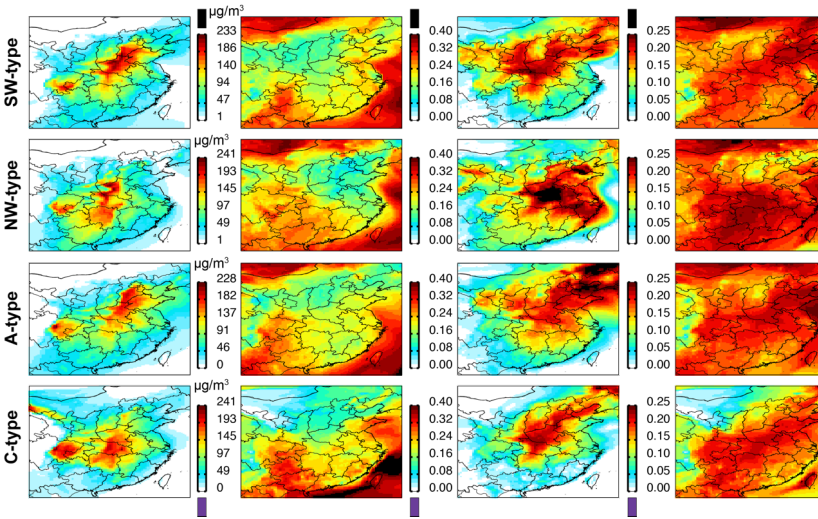


Figure S10 Spatial distribution of PM_{2.5} concentrations and the fraction of each inorganic salt (sulfate: second column; nitrate: third column; ammonium: forth column) to PM_{2.5} for these four typical heavy pollution processes simulated by GEOS-Chem control simulation.

Reference:

Cao, J.-J., Shen, Z.-X., Chow, J. C., Watson, J. G., Lee, S.-C., Tie, X.-X., Ho, K.-F., Wang, G.-H., and Han, Y.-M.: Winter and Summer PM_{2.5} Chemical Compositions in Fourteen Chinese Cities, *Journal of the Air & Waste Management Association*, 62, 1214-1226, 10.1080/10962247.2012.701193, 2012.

Huang, W., Cao, J., Tao, Y., Dai, L., Lu, S.-E., Hou, B., Wang, Z., and Zhu, T.: Seasonal Variation of Chemical Species Associated With Short-Term Mortality Effects of PM_{2.5} in Xi'an, a Central City in China, *American Journal of Epidemiology*, 175, 556-566, 10.1093/aje/kwr342, 2012.

Liu, Z., Gao, W., Yu, Y., Hu, B., Xin, J., Sun, Y., Wang, L., Wang, G., Bi, X., Zhang, G., Xu, H., Cong, Z., He, J., Xu, J., and Wang, Y.: Characteristics of PM_{2.5} mass concentrations and chemical species in urban and background areas of China: emerging results from the CARE-China network, *Atmospheric Chemistry and Physics*, 18, 8849-8871, 10.5194/acp-18-8849-2018, 2018.

Luo, Y., Zhou, X., Zhang, J., Xiao, Y., Wang, Z., Zhou, Y., and Wang, W.: PM_{2.5} pollution in a petrochemical industry city of northern China: Seasonal variation and source apportionment, *Atmospheric Research*, 212, 285-295, 10.1016/j.atmosres.2018.05.029, 2018.

Wang, H. L., Qiao, L. P., Lou, S. R., Zhou, M., Ding, A. J., Huang, H. Y., Chen, J. M., Wang, Q., Tao, S., Chen, C. H., Li, L., and Huang, C.: Chemical composition of PM_{2.5} and meteorological impact among three years in urban Shanghai, China, *Journal of Cleaner Production*, 112, 1302-1311, 10.1016/j.jclepro.2015.04.099, 2016a.

Wang, J., Li, X., Zhang, W., Jiang, N., Zhang, R., and Tang, X.: Secondary PM_{2.5} in Zhengzhou, China: Chemical Species Based on Three Years of Observations, *Aerosol and Air Quality Research*, 16, 91-104, 10.4209/aaqr.2015.01.0007, 2016b.

Wang, Q., Fang, J., Shi, W., and Dong, X.: Distribution characteristics and policy-related improvements of PM_{2.5} and its components in six Chinese cities, *Environmental Pollution*, 266, 10.1016/j.envpol.2020.115299, 2020.

Xu, Q., Wang, S., Jiang, J., Bhattarai, N., Li, X., Chang, X., Qiu, X., Zheng, M., Hua, Y., and Hao, J.: Nitrate dominates the chemical composition of PM_{2.5} during haze event in Beijing, China, *Science of the Total Environment*, 689, 1293-1303, 10.1016/j.scitotenv.2019.06.294, 2019.

Zhang, T., Cao, J. J., Tie, X. X., Shen, Z. X., Liu, S. X., Ding, H., Han, Y. M., Wang, G. H., Ho, K. F., Qiang, J., and Li, W. T.: Water-soluble ions in atmospheric aerosols measured in Xi'an, China: Seasonal variations and sources, *Atmospheric Research*, 102, 110-119, 10.1016/j.atmosres.2011.06.014, 2011.

Zheng, J., Hu, M., Peng, J., Wu, Z., Kumar, P., Li, M., Wang, Y., and Guo, S.: Spatial distributions and chemical properties of PM_{2.5} based on 21 field campaigns at 17 sites in China, *Chemosphere*, 159, 480-487, 10.1016/j.chemosphere.2016.06.032, 2016.

Minor comments:

Line 101-103: There must be many studies targeted the mitigation of PM_{2.5} at a regional scale (Ding et al., 2019; Zhang et al., 2019, Xing et al., 2018, 2019; Fu et al., 2017; etc.). Please rephrase this sentence.

We have rephrased this sentence: "Although there are many studies targeted PM_{2.5} mitigations at a regional scale (Ding et al., 2019; Zhang et al., 2019, Xing et al., 2018,

138 2019; Fu et al., 2017; etc.), their results can not be directly applied to reduce winter
139 PM_{2.5} pollution under various synoptic controls.”

140 Line 148-150: It is very confusing. The circulation classification is based on the
141 meteorological data from November 2013 to February 2014, which is also the
142 simulation episode. Why did you use the hourly PM_{2.5} data from 2013-2018?

143 We used the hourly PM_{2.5} from November 2013 to December 2018 to screen the
144 pollution days (daily mean PM_{2.5} larger than 150 µg/m³) and applied the daily mean sea
145 level pressure between 2013 and 2018 from the NCEP/NCAR FNL Operational Global
146 Analysis data to conduct the circulation classification. The meteorological observations
147 at Jingzhou from November 2013 to February 2014 are used to analyze the
148 meteorological characteristics during the period four severe particle pollution events
149 occurred in succession over Central China. We have revised the Sect. 2.1:

150 “Hourly mass concentrations of PM_{2.5} at Jingzhou (112.18°E, 30.33°N, 33.7 m)
151 from November 2013 to December 2018 are obtained from Hubei Environmental
152 Monitoring Central Station (<http://sthjt.hubei.gov.cn/>). We screen the pollution days
153 with daily mean PM_{2.5} concentrations larger than 150 µg/m³ for circulation
154 classification.

155 We use the daily mean sea level pressure (SLP) between 2013 and 2018 from the
156 National Centers for Environmental Prediction/National Center for Atmospheric
157 Research (NCEP/NCAR) Final (FNL) Operational Global Analysis data (horizontal
158 resolution: 1° × 1°; temporal resolution: 6 hours; <https://rda.ucar.edu/datasets/ds083.3/>)
159 to conduct the classification of Lamb-Jenkenson circulation types.

160 The meteorological data of surface observations at Jingzhou, including ambient
161 temperature, relative humidity, wind speed, wind direction and atmospheric pressure,
162 are obtained from Hubei Meteorological Information and Technology Support Center
163 (<http://hb.cma.gov.cn/qxfw/index.html>). The data from November 2013 to February
164 2014 are used to analyze the meteorological characteristics during the period four
165 severe particle pollution events occurred in succession over Central China (Fig. S1).”

166 Line 195: Did you do nested runs or just one domain covering China? Please make this

167 clear.

168 We have specified the model setups in the revised sentences: “The nested model,
169 covering China (70°E-140°E, 15°S-55°N), is run with a horizontal resolution of 0.25°
170 latitude × 0.3125° longitude and 72 vertical layers. The boundary condition of nested
171 model is provided by the GEOS-Chem global model with a horizontal resolution of 2°
172 latitude × 2.5° longitude (Fig. S3). Both global and nested simulations, driven by the
173 GEOS-FP assimilated meteorological data, include detailed tropospheric Ozone-NO_x-
174 VOCs-HO_x-aerosol chemistry.”

175 Line 205: The SEEA inventory was developed for the year 2017. Did you use it directly
176 without projection to the simulation episode? If you adjusted this inventory, what are
177 the factors applied for the PM_{2.5} precursors and how did you obtain those data?

178 Yes, we have used the SEEA inventory of the year 2017 directly without projection to
179 the simulation episode. The uncertainty discussion has been listed in Sect. 3.3:
180 “Anthropogenic emissions for PM_{2.5} precursors used here are for the year 2017 over
181 Central China from SEEA inventory (Table S4). From 2013 to 2017, anthropogenic
182 NO_x, SO₂, and primary PM_{2.5} emissions in Central China have declined substantially
183 (Table S4), due to implementation of stringent emission control measures for the 12th-
184 13th Five-Year Plans (Zheng et al., 2018). The anthropogenic emissions biases may
185 affect our simulations and PM_{2.5} attribution results to some extent.”

186 Line 215-217: Have you compared the modeled sulfate with observations, at least in
187 Jingzhou? How about the model performances of the other components of PM_{2.5}?

188 We have no observations of the chemical compositions of PM_{2.5}. In order to examine
189 the model performances in the PM_{2.5} chemical compositions, we have added Table 4 to
190 review the reported concentrations of PM_{2.5} and the three inorganic salts (sulfate, nitrate
191 and ammonium) in other cities. The contributions of sulfate, nitrate and ammonium are
192 9.1%-31.9%, 5.7%-32.1% and 5.9%-13.3%, respectively. In the CON simulation, the
193 fractions of each inorganic salt to PM_{2.5} for these four typical heavy pollution processes
194 are shown in revised Fig. S10, which are comparable to the previous observed results
195 (Table 4). Please see details in the response of major comment#4.

196 Line 305: Again, I am confused about the emissions used in the CON case. You listed
197 too many options for the anthropogenic source in Table S2. What inventories were
198 EXACTLY selected for the CON case? Did you do a global/regional nested run? Please
199 explain the choices of emissions in a separate column in the table.

200 We do a nested simulation, covering China (70°E-140°E, 15°S-55°N) with a horizontal
201 resolution of 0.25° latitude × 0.3125° longitude. The boundary condition of nested
202 model is provided by the GEOS-Chem global model with a horizontal resolution of 2°
203 latitude × 2.5° longitude (Fig. S3). The emission inventories for each domain are shown

204 in the revised Table S1 and Table S2. Please see details in the response of major
205 comment#2.

206 Line 310: Please compare the meteorological field used in the model with observations
207 to confirm that statement. Also, there are no perfect mechanisms, inventories, or
208 parameterization of the model with no doubt. I suggest using "uncertainties".

209 We thank the referee for this comment. In order to explain the causes of the model
210 discrepancy, we have added Table S3 to show the observed (modeled) meteorological
211 conditions averaged over these four pollution episodes controlled by SW-type, NW-
212 type, A-type and C-type synoptic pattern, respectively. There is an overestimate in
213 temperature and wind speed and an underestimate in humidity, which can partly
214 contribute to the underestimation of modeled PM_{2.5} concentrations. In addition,
215 anthropogenic emissions for PM_{2.5} precursors used here are for the year 2017 over
216 Central China from SEEA inventory (Table S4). From 2013 to 2017, anthropogenic
217 NO_x, SO₂, and primary PM_{2.5} emissions in Central China have declined substantially
218 (Table S4), due to implementation of stringent emission control measures for the 12th-
219 13th Five-Year Plans (Zheng et al., 2018). The anthropogenic emissions biases may
220 affect our simulations and PM_{2.5} attribution results to some extent. Additionally, the
221 underestimation is on a national scale when compared with the MEE observations, with
222 a bias of -29.3 μg/m³, -18.7 μg/m³, -39.0 μg/m³ and -21.4 μg/m³ on average for SW-
223 type, NW-type, A-type and C-type synoptic pattern, respectively (Fig. 6). The national
224 negative biases may be also attributed to insufficient resolution of the model (Yan et
225 al., 2014) and imperfect chemical mechanisms (Yan et al., 2019). Please see details in
226 the response of major comment#4.

227 Line 323-324: A comparison of the modeled fractions of the inorganic salts to
228 observations, or reported values from other literature if no measurements are available.

229 We have no observations of the chemical compositions of PM_{2.5}. In order to examine
230 the model performances in the PM_{2.5} chemical compositions, we have added Table 4 to
231 review the reported concentrations of PM_{2.5} and the three inorganic salts (sulfate, nitrate
232 and ammonium) in other cities. The contributions of sulfate, nitrate and ammonium are
233 9.1%-31.9%, 5.7%-32.1% and 5.9%-13.3%, respectively. In the CON simulation, the
234 fractions of each inorganic salt to PM_{2.5} for these four typical heavy pollution processes
235 are shown in revised Fig. S10, which are comparable to the previous observed results
236 (Table 4). Please see details in the response of major comment#4.

237 Line 324: "As shown in Table 3,"

238 Modified.

239 Line 358: How was this calculated? Please explain it.

240 We have added the explanation in the revised sentence: "In addition, the contributions

241 from transboundary transport from non-Jingzhou Central China is simulated to be 12.0%
242 by comparing the results of XJ0 and XCC0.”

243 Line 415-417: How about the contributions of transported pollutants to the chemical
244 composition of PM_{2.5} under the four PSCs?

245 We have discussed in the revised Sect. 3.4. During the pollution episodes of
246 transmission-pollution characteristics (SW/NW-type), the contribution of transported
247 pollutants to the chemical composition of PM_{2.5} is significant. For the SW-type synoptic
248 controlled pollution event, the transport of air pollutants from the south leads to the
249 smallest proportion of the three inorganic salts (45.7%) in Jingzhou among the four
250 pollution episodes (50.3%-55.5% for other three episodes), because the emissions of
251 SO₂, NO₂ and NH₃ in the south (especially in Guangxi and Guizhou province) are
252 smaller than those in Central China (Li et al., 2017a). However, during the NW-type
253 synoptic controlled pollution episode, due to the transport contribution of pollutants
254 from northern China (with much higher anthropogenic emissions of SO₂, NO₂ and NH₃)
255 (Li et al., 2017a), the total proportion of the three inorganic salts is the highest (55.5%).
256 For the other two types (A/C-type) synoptic controlled pollutions, local emission
257 sources dominate the contributions and the contributions of transported pollutants to
258 the chemical composition of PM_{2.5} are small.

259 Line 424: The base year of emission reduction is 2015 for the 13th Five-year plan,
260 which is quite different from your inventory. How effective is the designed reduction
261 ratio of the anthropogenic emissions in this study?

262 Although the base year of emission reduction is 2015 for the 13th Five-year plan, it does
263 not affect to use the simulation results of emission scenarios (with the reduction ratio
264 of 20% applied to the simulated year 2013/2014) to explore the emission reduction
265 effect of specific haze pollution events. We have added this illustration in the revised
266 Sect. 3.5.

267 Line 425 and 428-429: Please explain these abbreviations in the text as well.

268 We have revised these sentences as: “The differences in model results between CON
269 (control simulation) and JSN/JSNN/JALL (emissions of
270 (SO₂+NO_x)/(SO₂+NO_x+NH₃)/all pollution sources at Jingzhou are reduced by 20%)
271 represent the environmental benefits caused by different local emission reduction
272 scenarios. The potential PM_{2.5} mitigations by joint prevention and control in different
273 regions are calculated by sensitivity experiments of CCALL (emissions of all pollution
274 sources over Central China are reduced by 20%), CNALL (over Central China and NCP
275 region), CPALL (over Central China and PRD region) and TALL (over Central China,
276 NCP, YRD, PRD and SCB regions).”

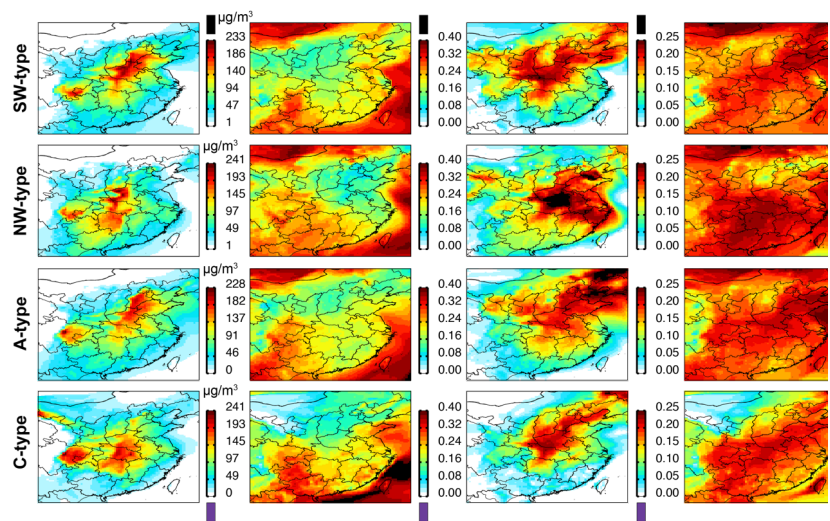
277 Line 437: I think an evaluation of the model performance in ammonium and/or

278 ammonia is desired to confirm that.

279 We thank the referee for this comment. We have no observations of the chemical
 280 compositions of PM_{2.5}. Thus we have removed this statement in the revised text.

281 Figure 6, 8, 9, 10: I suggest to show the fraction of each inorganic salt to PM_{2.5} rather
 282 than their total mass.

283 We have shown the fraction of each inorganic salt to PM_{2.5} in the revised Fig. S10.



285 Figure S10 Spatial distribution of PM_{2.5} concentrations and the fraction of each
 286 inorganic salt (sulfate: second column; nitrate: third column; ammonium: forth column)
 287 to PM_{2.5} for these four typical heavy pollution processes simulated by GEOS-Chem
 288 control simulation.

289 Figure 11. It should be “TALL” in NW and C.

290 Modified.

291 References:

292 Wenyan Chang and Jianqiong Zhan, The association of weather patterns with haze
 293 episodes: Recognition by PM_{2.5} oriented circulation classification applied in Xiamen,
 294 Southeastern China, Atmospheric Research, 197, 425-436, 2017.

295 Huibin Dai, Jia Zhu, Hong Liao, Jiandong Li, Muxue Liang, Yang Yang, Xu Yue, Co-
 296 occurrence of ozone and PM_{2.5} pollution in the Yangtze River Delta over 2013–2019:
 297 Spatiotemporal distribution and meteorological conditions, *Atmospheric Research*, 249,
 298 105363, 2021.

299 Qiang Zhang, Yixuan Zheng, Dan Tong, et al., Drivers of improved PM_{2.5} air quality
 300 in China from 2013 to 2017, *Proceedings of the National Academy of Sciences*, 116
 301 (49) 24463-24469, 2019.

302 Aijun Ding, Xin Huang, Wei Nie, et al., Significant reduction of PM_{2.5} in eastern China
 303 due to regional-scale emission control: evidence from SORPES in 2011–2018,
 304 *Atmospheric Chemistry and Physics*, 19, 11791– 11801, 2019.

305 Xing, J., Ding, D., Wang, S., Dong, Z., Kelly, J. T., Jang, C., ... & Hao, J. Development
 306 and application of observable response indicators for design of an effective ozone and
 307 fine-particle pollution control strategy in China. *Atmospheric Chemistry & Physics*,
 308 19(21), 2019.

309 Xing, J., Ding, D., Wang, S., Zhao, B., Jang, C., Wu, W., ... & Hao, J. Quantification
 310 of the enhanced effectiveness of NO_x control from simultaneous reductions of VOC
 311 and NH₃ for reducing air pollution in the Beijing–Tianjin–Hebei region, China.
 312 *Atmospheric Chemistry and Physics*, 18(11), 7799-7814, 2018.

313 Fu, X., Wang, S., Xing, J., Zhang, X., Wang, T., & Hao, J. Increasing ammonia
 314 concentrations reduce the effectiveness of particle pollution control achieved via SO₂
 315 and NO_x emissions reduction in east China. *Environmental Science & Technology*
 316 *Letters*, 4(6), 221-227, 2017.

317

318

319

320

321

322

323 =====

324 Response to the Second Referee

325 =====

326 Reviewer #2:

327 This article analyses the potential synoptic controls over central China during winter
328 haze pollution episodes by using Lamb-Jenkenson method and the NCEP/NCAR FNL
329 operational global analysis data, and further evaluates the effectiveness of emission
330 control to reduce PM_{2.5} under main synoptic conditions by GEOS-Chem model
331 simulations. They found a substantial contribution of transportation in two synoptic
332 patterns (SW-type and NW-type) and a dominated contribution of local emission
333 sources in other two synoptic conditions (A-type and C-type). These results provide an
334 opportunity to effectively mitigate haze pollution by local emission control actions in
335 coordination with regional collaborative actions according to different synoptic patterns.
336 The topic is of practical significance and the results are reliable. I would suggest for
337 publication after addressing my comments below.

338 We thank the reviewer for comments, which have been incorporated to improve the
339 manuscript.

340 1. The present comparison and verification of control simulation results in GEOS-Chem
341 is not enough. It can be further verified by using PM_{2.5} observation data in a larger
342 region of China or component observations of PM_{2.5} at some specific sites.

343 We thank the referee for his/her reading of our manuscript. The comments and
344 suggestions are valuable for us to improve our work.

345 In order to better evaluate the GEOS-Chem model performances, the spatial distribution
346 of PM_{2.5} concentrations averaged over the four typical heavy pollution processes
347 simulated by the control (CON) simulation are compared with the observations (a total
348 of 633 sites) from Ministry of Ecology and Environment of China
349 (<http://www.mee.gov.cn/>) (revised Fig. 6). Similar to the underestimation in PM_{2.5} at
350 Jingzhou, the underestimation is on a national scale when compared with the MEE
351 observations, with a bias of -29.3 µg/m³, -18.7 µg/m³, -39.0 µg/m³ and -21.4 µg/m³ on
352 average for SW-type, NW-type, A-type and C-type synoptic pattern, respectively (Fig.
353 6).

354 We have no observations of the chemical compositions of PM_{2.5}. In order to examine
355 the model performances in the PM_{2.5} chemical compositions, we have added Table 4 to
356 review the reported concentrations of PM_{2.5} and the three inorganic salts (sulfate, nitrate

and ammonium) in other cities. The contributions of sulfate, nitrate and ammonium are 9.1%-31.9%, 5.7%-32.1% and 5.9%-13.3%, respectively. In the CON simulation, the fractions of each inorganic salt to PM_{2.5} for these four typical heavy pollution processes are shown in revised Fig. S10, which are comparable to the previous observed results (Table 4).

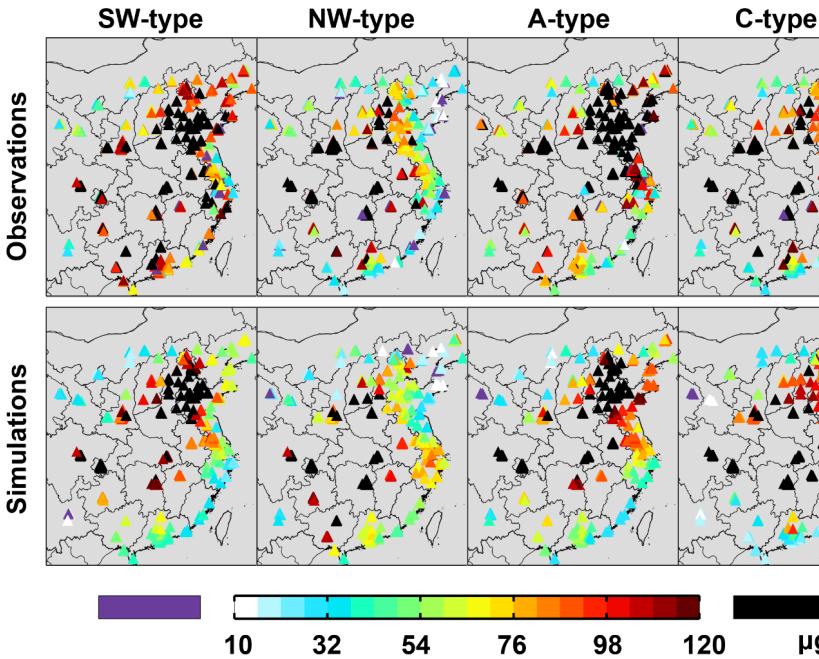


Figure 6 Spatial distribution of observed (top row) and modeled (bottom row, by CON case) PM_{2.5} concentrations (µg/m³) averaged over four severe pollution episodes controlled by SW-type (first column), NW-type (second column), A-type (third column) and C-type (forth column) synoptic pattern, respectively.

Table 4 The reported concentrations of PM_{2.5} and the three inorganic salts (sulfate, nitrate and ammonium, µg/m³) in other cities.

References	Site	Time	PM _{2.5}	Sulfate	Nitrate	Ammonium
Cao et al., 2012	Beijing	01/03	115.6±46.6	20.0±4.2 (17.3%)	13.1±4.5 (11.3%)	9.4±4.1 (8.1%)

Cao et al., 2012	Qingdao	01/03	134.8±43.0	21.1±7.7 (15.7%)	19.3±9.2 (14.3%)	15.3±5.2 (11.4%)
Cao et al., 2012	Tianjin	01/03	203.1±76.2	32.5±15. (16.0%)	25.2±10. (12.4%)	22.2±9.8 (10.9%)
Cao et al., 2012	Xi'an	01/03	356.3±118. 4	53.8±25. 6 (15.1%)	29.0±10. 0 (8.1%)	29.8±11.5 (8.4%)
Cao et al., 2012	Chongqing	01/03	316.6±101. 2	60.9±19. 6 (19.2%)	18.1±6.4 (5.7%)	28.8±8.9 (9.1%)
Cao et al., 2012	Hangzhou	01/03	177.3±59.5	33.4±16. (18.8%)	25.7±14. (14.5%)	19.1±10.7 (10.8%)
Cao et al., 2012	Shanghai	01/03	139.4±50.6	21.6±12. 3 (15.5%)	17.5±8.7 (12.6%)	14.5±5.9 (10.4%)
Cao et al., 2012	Wuhan	01/03	172.3±67.0	31.4±15. 6 (18.2%)	22.2±10. 7 (12.9%)	18.4±10.2 (10.7%)
Zhang et al., 2011	Xi'an	03/06-03/07	194.1	35.6 (18.3%)	16.4 (8.4%)	11.4 (5.9%)
Huang et al., 2012	Xi'an	01/06-02/06	235.8±125. 1	44.8±31. 3 (19.0%)	20.5±14. 2 (8.7%)	14.5±10.8 (6.1%)
Wang et al., 2020	Jinan	10/17	104±54	14.4±9.2 (13.8%)	33.4±23. 2 (32.1%)	13.0±8.3 (12.5%)

				19.3±19.6	42.8±41.1	
Wang et al., 2020	Shijiazhuang	10/17	152±109	6	1	18.2±17.1 (12.0%)
				(12.7%)	(28.2%)	
Wang et al., 2020	Wuhan	12/17	117±33	13.6±3.2	26.6±11.1	13.1±3.8 (11.2%)
				(11.6%)	(22.7%)	
Wang et al., 2016a	Zhengzhou	01/11-02/11	297±160	48±36	31±19	21±16 (7.1%)
				(16.2%)	(10.4%)	
Wang et al., 2016a	Zhengzhou	01/12-02/12	234±125	23±10	22±9	16±5 (6.8%)
				(9.8%)	(9.4%)	
Wang et al., 2016a	Zhengzhou	01/13-02/13	337±168	56±39	39±20	31±18 (9.2%)
				(16.6%)	(11.6%)	
Luo et al., 2018	Zibo	12/06-02/07	224.9±85.4	40.1±19.2	18.1±9.0	21.7±10.2 (9.7%)
				(17.9%)	(8.1%)	
Wang et al., 2016b	Shanghai	12/11, 12/12, 12/13	73.9±57.5	12.2±9.2	14.6±12.2	8.2±6.7 (11.1%)
				(16.5%)	(19.8%)	
Xu et al., 2019	Beijing	02/17-03/17	180.5	20.1	45.6	22.5 (12.5%)
				(11.1%)	(25.3%)	
Xu et al., 2019	Beijing	05/17-09/17	186.7	20.2	32.4	17.1 (9.2%)
				(10.8%)	(17.4%)	
Xu et al., 2019	Beijing	10/17-11/17	167.5	17.9	44.5	20.9 (12.5%)
				(10.7%)	(26.6%)	
Zheng et al., 2016	Beijing	03/10-05/10	65.2±65.1	11.1±10.1	11.1±11.1	6.8±6.7 (10.4%)
				(17.0%)	(17.0%)	

				23.0±13.9	16.2±11.8	11.8±6.8
Zheng et al., 2016	Beijing	07/09-08/09	88.9±39.1	(25.9%)	(18.2%)	(13.3%)
Zheng et al., 2016	Beijing	12/09-02/10	84.0±66.6	(9.1%)	(9.0%)	(6.6%)
Zheng et al., 2016	Guangzhou	11/10	73.3±16.5	(22.6%)	(7.8%)	(8.5%)
Zheng et al., 2016	Shenzhen	12/09	64.6±24.7	(31.9%)	(7.6%)	(7.1%)
Zheng et al., 2016	Wuxi	04/10-05/10	82.1±27.0	(15.6%)	(12.1%)	(8.5%)
Zheng et al., 2016	Jinhua	10/11-11/11	81.9±26.2	(22.3%)	(15.4%)	(12.7%)
Liu et al., 2018	Chongqing	2012-2013	73.5±30.5	(26.8%)	(8.8%)	(8.3%)
Liu et al., 2018	Shanghai	2012-2013	68.4±20.3	(19.9%)	(17.4%)	(8.5%)
Liu et al., 2018	Beijing	2012-2013	71.7±36.0	(16.6%)	(13.0%)	(7.4%)

Reference:

- Cao, J.-J., Shen, Z.-X., Chow, J. C., Watson, J. G., Lee, S.-C., Tie, X.-X., Ho, K.-F., Wang, G.-H., and Han, Y.-M.: Winter and Summer PM_{2.5} Chemical Compositions in Fourteen Chinese Cities, Journal of the Air & Waste Management Association, 62, 1214-1226, 10.1080/10962247.2012.701193, 2012.
- Huang, W., Cao, J., Tao, Y., Dai, L., Lu, S.-E., Hou, B., Wang, Z., and Zhu, T.: Seasonal Variation of Chemical Species Associated With Short-Term Mortality Effects of PM_{2.5} in Xi'an, a Central City in China, American Journal of Epidemiology, 175, 556-566, 10.1093/aje/kwr342, 2012.
- Liu, Z., Gao, W., Yu, Y., Hu, B., Xin, J., Sun, Y., Wang, L., Wang, G., Bi, X., Zhang, G., Xu, H., Cong, Z., He, J., Xu, J., and Wang, Y.: Characteristics of PM_{2.5} mass concentrations and chemical species in urban and background areas of China: emerging results from the CARE-China network,

381 Atmospheric Chemistry and Physics, 18, 8849-8871, 10.5194/acp-18-8849-2018, 2018.

382 Luo, Y., Zhou, X., Zhang, J., Xiao, Y., Wang, Z., Zhou, Y., and Wang, W.: PM_{2.5} pollution in a
383 petrochemical industry city of northern China: Seasonal variation and source apportionment,
384 Atmospheric Research, 212, 285-295, 10.1016/j.atmosres.2018.05.029, 2018.

385 Wang, H. L., Qiao, L. P., Lou, S. R., Zhou, M., Ding, A. J., Huang, H. Y., Chen, J. M., Wang, Q.,
386 Tao, S., Chen, C. H., Li, L., and Huang, C.: Chemical composition of PM_{2.5} and meteorological
387 impact among three years in urban Shanghai, China, Journal of Cleaner Production, 112, 1302-
388 1311, 10.1016/j.jclepro.2015.04.099, 2016a.

389 Wang, J., Li, X., Zhang, W., Jiang, N., Zhang, R., and Tang, X.: Secondary PM_{2.5} in Zhengzhou,
390 China: Chemical Species Based on Three Years of Observations, Aerosol and Air Quality Research,
391 16, 91-104, 10.4209/aaqr.2015.01.0007, 2016b.

392 Wang, Q., Fang, J., Shi, W., and Dong, X.: Distribution characteristics and policy-related
393 improvements of PM_{2.5} and its components in six Chinese cities, Environmental Pollution, 266,
394 10.1016/j.envpol.2020.115299, 2020.

395 Xu, Q., Wang, S., Jiang, J., Bhattarai, N., Li, X., Chang, X., Qiu, X., Zheng, M., Hua, Y., and Hao,
396 J.: Nitrate dominates the chemical composition of PM_{2.5} during haze event in Beijing, China,
397 Science of the Total Environment, 689, 1293-1303, 10.1016/j.scitotenv.2019.06.294, 2019.

398 Zhang, T., Cao, J. J., Tie, X. X., Shen, Z. X., Liu, S. X., Ding, H., Han, Y. M., Wang, G. H., Ho, K.
399 F., Qiang, J., and Li, W. T.: Water-soluble ions in atmospheric aerosols measured in Xi'an, China:
400 Seasonal variations and sources, Atmospheric Research, 102, 110-119,
401 10.1016/j.atmosres.2011.06.014, 2011.

402 Zheng, J., Hu, M., Peng, J., Wu, Z., Kumar, P., Li, M., Wang, Y., and Guo, S.: Spatial distributions
403 and chemical properties of PM_{2.5} based on 21 field campaigns at 17 sites in China, Chemosphere,
404 159, 480-487, 10.1016/j.chemosphere.2016.06.032, 2016.

405 2. The novelty of this study need to be further clarified. New understanding or
406 improvement of conclusion and application or in methods should be provided to reflect
407 the general interests of the work rather than the local interests.

408 In Sect.1, we have further clarified and provided support that significant and new
409 scientific merits are presented in this work. The PM_{2.5} pollution in China has been
410 continuously alleviating since 2013 as the implication of the Air Pollution Prevention
411 and Control Action Plan. However, severe particle pollution still occurs frequently in
412 autumn and winter, which is the major reason restricting the PM_{2.5} to come up to
413 national standard. Currently, how to effectively reduce emissions in autumn and winter
414 is the key to mitigate haze pollution in China. Previous studies have highlighted that
415 different levels of PM_{2.5} pollutions are closely related to the dominant synoptic patterns
416 in different regions, and they attribute the large spatial variability of pollution to the

regional transport contributions, not only the different local sources of PM_{2.5}. Thus, heavy pollution prevention and control needs to consider the weather situation, otherwise local emission reduction measures would not work well. However, under different synoptic conditions, how to effectively reduce local and regional emissions to control haze pollution is rarely reported. In order to investigate the effectiveness of emission control to reduce PM_{2.5} pollution under various potential synoptic controls, we take the severe particle pollution of winter haze episodes over Central China with transmission-pollution characteristics as an example. This study combines the atmospheric (circulation classification) and environmental (chemical transport modeling) research methods and could provide reference for emission control of severe winter haze pollution under different weather types, and provide basis for regional air quality policy-making.

3. Lines 105-109: several studies have investigated the potential effective emission reduction on ammonia, which should be reviewed here properly.

We have added the review of studies on potential efficiency of ammonia emission reduction in alleviating particulate pollution: “Moreover, current emission reduction policies in China mainly aimed at sulfur dioxide (SO₂) and nitrogen dioxide (NO₂), ignoring the effective emission reduction on ammonia (NH₃), although some modeling works have discussed the effectiveness of ammonia emission reduction for PM_{2.5} mitigations (Liu et al., 2019; Ye et al., 2019; Xu et al., 2019; Bai et al., 2019).”

Bai, Z., Winiwarter, W., Klimont, Z., Velthof, G., Misselbrook, T., Zhao, Z., Jin, X., Oenema, O., Hu, C., and Ma, L.: Further Improvement of Air Quality in China Needs Clear Ammonia Mitigation Target, *Environmental Science & Technology*, 53, 10542-10544, 10.1021/acs.est.9b04725, 2019.

Liu, M., Huang, X., Song, Y., Tang, J., Cao, J., Zhang, X., Zhang, Q., Wang, S., Xu, T., Kang, L., Cai, X., Zhang, H., Yang, F., Wang, H., Yu, J. Z., Lau, A. K. H., He, L., Huang, X., Duan, L., Ding, A., Xue, L., Gao, J., Liu, B., and Zhu, T.: Ammonia emission control in China would mitigate haze pollution and nitrogen deposition, but worsen acid rain, *Proceedings of the National Academy of Sciences of the United States of America*, 116, 7760-7765, 10.1073/pnas.1814880116, 2019.

Xu, Z., Liu, M., Zhang, M., Song, Y., Wang, S., Zhang, L., Xu, T., Wang, T., Yan, C., Zhou, T., Sun, Y., Pan, Y., Hu, M., Zheng, M., and Zhu, T.: High efficiency of livestock ammonia emission controls in alleviating particulate nitrate during a severe winter haze episode in northern China, *Atmospheric Chemistry and Physics*, 19, 5605-5613, 10.5194/acp-19-5605-2019, 2019.

Ye, Z., Guo, X., Cheng, L., Cheng, S., Chen, D., Wang, W., and Liu, B.: Reducing PM_{2.5} and secondary inorganic aerosols by agricultural ammonia emission mitigation within the Beijing-Tianjin-Hebei region, China, *Atmospheric Environment*, 219,

4. In Section 3.2, the mechanisms of heavy particle pollution caused by these four potential synoptic controls should be briefly discussed when describe characteristics of each synoptic pattern.

We have briefly discussed the mechanisms of heavy particle pollution caused by the four PSCs in the revised Section 3.2, when describe characteristics of each synoptic pattern:

“SW-type circulation is the predominant PSC of severe PM_{2.5} pollution episodes. The circulation at 500 hPa is relatively flat and the whole East Asia region is affected by the westerly flow (Fig. S6a). Westerly belt fluctuates greatly at 700 hPa and there are two ridges and a southwest trough in the middle latitudes of Asia (Fig. S7a). Jingzhou is located in the front of a trough, prevailing the weak southwest airflow. At 850 hPa, the cold high pressure center is formed in Xinjiang of China. Warm low pressure appears in the low latitude area and weak high pressure appears in the East China Sea (Fig. 3a). In combination with the surface field, a high-low-high saddle like field forms from west to east (Fig. 4a). Such synoptic type is also the dominant weather system of eastern China (Shu et al., 2017; Yang et al., 2018). Jingzhou is located in the back of Bohai-northeast high pressure and the front of southwest warm low pressure. Thus it is affected by the southerly airflow, which could be conducive to the transport of air pollutants formed over southern China to Central China. Associated with small local surface wind speed (< 3 m/s) at Jingzhou, the dispersion of local and transported pollutants is inhibited.

NW-type circulation mainly occurs in the early winter (December and January). This synoptic pattern is also reported as one of the main types to affect the aerosol distributions over eastern China (Zheng et al., 2015). Circulation at 500 hPa is controlled by one trough and one ridge, with the weak ridge located in the northwest of China and the shallow trough located in the northeast of China (Fig. S6b). The whole East Asia is affected by the westerly current. The trough and ridge at 700 hPa are deepened. Jingzhou is located at the bottom of the shallow trough, prevailing the west-northwest airflow, affected by the flow around the plateau (Fig. S7b). At 850 hPa, the cold high pressure center is formed in Xinjiang, and Jingzhou is affected by the northerly airflow, due to being in the front of the high pressure (Fig. 3b). For the sea level pressure, the cold high pressure is located in the west of Mongolia and Xinjiang of China (Fig. 4b). Jingzhou is located at the region with weak fluctuation in the front of the high pressure, and the surface wind speed is smaller than 2 m/s. The haze episodes induced by NW-type synoptic pattern is similar to the transmission-accumulation pollution caused by SW-type, but the transmission path is from Northern China to Central China.

A-type circulation also mainly occurs in the early winter. The high-altitude circulation field is controlled by one trough and one ridge (Fig. S6c and S7c). East Asia

is affected by west-northwest air flow, and the SLP is controlled by a huge high pressure, with the center located in the southwest of Baikal Lake (Fig. 4c). A surface high pressure favors the accumulation of air pollutants, especially over the regions of high pressure center (Leung et al., 2018). Jingzhou is in the sparse pressure field in front of the high pressure (Fig. 3c and 4c), with an average surface wind speed of ~1.3 m/s. The uniform west-northwest air flow at high altitude would lead to the low water vapor content and less cloud amount, which is conducive to radiation cooling at night. In addition, due to the weak high pressure ridge in the north, it is not conducive to the eastward and southward movement of cold air, leading to the stable weather situation and thus severe haze pollution at Jingzhou. This type is also responsible for most of the severe particulate pollution days in the BTH and YRD regions (Li et al., 2019).

C-type circulation mainly occurs in late winter and early spring, when the relative humidity is large with an average value of 74%. East Asia is controlled by the straight westerly flow, and the southwest shallow trough is obvious at 500 hPa (Fig. S6d). Additionally, the West Pacific subtropical high extends to the west, Central China is affected by the southwest flow. Southwest trough is deepened at 700 hPa, and Jingzhou is located in front of the trough and controlled by the southwest airflow (Fig. S7d). High pressure at the south of Xinjiang and the north of Plateau is strengthened at 850 hPa, and the southwest low pressure center is formed (Fig. 3d). Jingzhou is located in the low pressure system on the SLP field (Fig. 4d), with small surface wind speed (0-3 m/s). Together with the large relative humidity, which can promote the hygroscopic growth of particulate matter (Twohy et al., 2009; Zheng et al., 2015), the haze pollution is persistent and serious at Jingzhou. The impact of low-pressure systems on winter heavy air pollution have also been reported in the northwest Sichuan Basin (Ning et al., 2018)."

5. Lines 294-296: Why the four pollution episodes are selected?

We have explained in the revised sentences: "In order to reduce the simulation cost, the continuous four severe haze episodes occurred during November, 2013-February, 2014 are selected. These four haze episodes are controlled by the synoptic pattern of SW-type (18-25 November, 2013), NW-type (19-26 December, 2013), A-type (14-21 January, 2014) and C-type (26 January - 2 February, 2014), respectively."

6. Lines 304-308: The model control simulation is compared to PM_{2.5} observations at just one site (Jingzhou). Current comparison is insufficient to demonstrate the modeling performance.

In order to better evaluate the GEOS-Chem model performances, the spatial distribution of PM_{2.5} concentrations averaged over the four typical heavy pollution processes simulated by the control (CON) simulation are compared with the observations (a total of 633 sites) from Ministry of Ecology and Environment of China (<http://www.mee.gov.cn/>) (revised Fig. 6). Please see details in the response of comment#1.

7. Line 308-311: Model biases are generally attributed to resolution, emission errors, meteorology and chemical mechanism without statistical results of further sensitivity simulations. Be careful to discuss the model deviation.

In order to explain the causes of the model discrepancy, we have added Table S3 to show the observed (modeled) meteorological conditions averaged over these four pollution episodes controlled by SW-type, NW-type, A-type and C-type synoptic pattern, respectively. There is an overestimate in temperature and wind speed and an underestimate in humidity, which can partly contribute to the underestimation of modeled PM_{2.5} concentrations. In addition, anthropogenic emissions for PM_{2.5} precursors used here are for the year 2017 over Central China from SEEA inventory (revised Table S4). From 2013 to 2017, anthropogenic NO_x, SO₂, and primary PM_{2.5} emissions in Central China have declined substantially (revised Table S4), due to the implementation of stringent emission control measures for the 12th-13th Five-Year Plans (Zheng et al., 2018). The anthropogenic emissions biases may affect our simulations and PM_{2.5} attribution results to some extent. Additionally, the underestimation is on a national scale when compared with the MEE observations, with a bias of -29.3 µg/m³, -18.7 µg/m³, -39.0 µg/m³ and -21.4 µg/m³ on average for SW-type, NW-type, A-type and C-type synoptic pattern, respectively (revised Fig. 6, see figure in the response of comment#1). The national negative biases may be also attributed to insufficient resolution of the model (Yan et al., 2014) and imperfect chemical mechanisms (Yan et al., 2019).

Table S3. The observed (modeled) meteorological conditions at Jingzhou averaged over these four pollution episodes controlled by SW-type, NW-type, A-type and C-type synoptic pattern, respectively.

PSC	Temperature (°C)	Humidity (%)	Pressure (kpa)	Wind speed (m/s)
SW	11.79 (12.96)	75.33 (69.25)	1018.33 (1024.06)	2.13 (3.09)
NW	3.61 (6.34)	71.16 (62.78)	1027.53 (1031.53)	1.44 (2.45)
A	5.81 (7.52)	64.96 (60.38)	1026.63 (1028.66)	1.45 (2.27)
C	9.60 (13.08)	78.10 (71.40)	1011.48 (1014.24)	1.88 (3.11)

Table S4. The emission amount of PM_{2.5} precursors over Central China calculated from SEEA (for the year 2017) and MEIC (for the years of 2013, 2014 and 2017) inventory (unit: 10⁴ ton).

Category	SO ₂	NO _x	NH ₃	PM _{2.5}	CO	BC	OC	VOCs
SEEA (2017)	48.4	94.0	54.6	26.4	553.8	6.2	12.9	117.2
MEIC (2017)	52.0	70.4	57.5	35.2	629.2	6.8	11.7	116.4
MEIC (2013)	173.3	98.4	62.4	54.5	836.5	9.2	16.7	116.6
MEIC (2014)	97.0	80.0	61.1	46.8	744.2	8.3	15.3	116.4

564

565 8. Line 337: PSC -> PSCs

566 [Modified.](#)

567 9. Line 359: The transportation of air pollutants from the south makes the proportion of
568 the three inorganic salts (45.7%) in Jingzhou area the smallest. Consider revising it like:
569 The transport of air pollutants from the south leads to the smallest proportion of the
570 three inorganic salts (45.7%) in Jingzhou.

571 [Modified.](#)

572 10. Line 482: remove potential synoptic controls or (PSC)

573 [Modified.](#)

574 11. Line 494: contribute 82%/85% of PM_{2.5}. Consider revising it like: dominate the
575 contribution (82%/85%) to PM_{2.5}.

576 [Modified.](#)

577

578

579

580

581

582

583

584

585

Effectiveness of emission control to reduce PM_{2.5} pollution of Central China during winter haze episodes under various potential synoptic controls

Yingying Yan ^{1#}, Yue Zhou ^{2#}, Shaofei Kong ^{1,4*}, Jintai Lin ³, Jian Wu ^{1,4}, Huang Zheng ^{1,4}, Zexuan Zhang ^{1,4}, [Aili Song ¹](#), Yongqing Bai ², Zhang Ling ², Dantong Liu ⁵, Tianliang Zhao ⁶

¹ Department of Atmospheric Sciences, School of Environmental Studies, China University of Geosciences, Wuhan, 430074, China

² Hubei Key Laboratory for Heavy Rain Monitoring and Warning Research, Institute of Heavy Rain, China Meteorological Administration, Wuhan 430205, China

³ Laboratory for Climate and Ocean-Atmosphere Studies, Department of Atmospheric and Oceanic Sciences, School of Physics, Peking University, Beijing 100871, China

⁴ Department of Environmental Science and Engineering, School of Environmental Studies, China University of Geosciences, Wuhan, 430074, China

⁵ Department of Atmospheric Sciences, School of Earth Sciences, Zhejiang University, Hangzhou, Zhejiang, China

⁶ School of Atmospheric Physics, Nanjing University of Information Science and Technology, Nanjing, 210044, China

Correspondence to: Shaofei Kong (kongshaofei@cug.edu.cn)

[#] Contributed equally to this work

Abstract

Currently [mitigating](#) the severe particle pollution in autumn and winter is the key to further improve the air quality of China. The source contributions and transboundary transport of fine particles (PM_{2.5}) in pollution episodes are closely related to large-scale or synoptic-scale atmospheric circulation. Under different synoptic conditions, how to effectively reduce emissions to control haze pollution is rarely reported. In this study, we classify the synoptic conditions over Central China from 2013 to 2018 by using

Deleted: solving

616 Lamb-Jenkenson method and the NCEP/NCAR FNL operational global analysis data.
 617 The effectiveness of emission control to reduce PM_{2.5} pollution during winter haze
 618 episodes under potential synoptic controls is simulated by GEOS-Chem model. Among
 619 the ten identified synoptic patterns, four types account for 87% of the total pollution
 620 days. Two typical synoptic modes of them are characterized by small surface wind
 621 speed and stable weather conditions/high relative humidity (A/C-type) over Central
 622 China due to a high-pressure system/a southwest trough low-pressure system, blocking
 623 pollutants dispersion. Sensitivity simulations show that these two heavy pollution
 624 processes are mainly contributed by local emission sources with ~82% for A-type and
 625 ~85% for C-type, respectively. The other two patterns lead to pollution of transport
 626 characteristics affected by northerly/southerly winds (NW/SW-type), carrying air
 627 pollution from northern/southern China to Central China. The contribution of pollution
 628 ~~transmission~~ from North/South China is 36.9%/7.6% of PM_{2.5} and local emission
 629 sources contribute 41%/69%. We also estimate the effectiveness of emission reduction
 630 in these four typical severe pollution synoptic processes. By only reducing SO₂ and
 631 NO_x emission and not controlling NH₃, the enhanced nitrate counteracts the effect of
 632 sulfate reduction on PM_{2.5} mitigations₂ with less than 4% decrease in PM_{2.5}. In addition,
 633 to effectively mitigate haze pollution ~~of~~ NW/SW-type synoptic controlled episodes,
 634 local emission control actions should be in coordination with regional collaborative
 635 actions.

Deleted: ation

Deleted: transport

Deleted: ation

Deleted: in

637 1 Introduction

638 The regional pollution of fine particles (PM_{2.5}) has attracted worldwide attention
 639 in the public and in the scientific community (Cheng et al., 2016; Li et al., 2017c; Lin
 640 et al., 2018; Bi et al., 2019) due to its detrimental effect on visibility (Wang et al., 2020)
 641 and public health (Agarwal et al., 2017; Zhang et al., 2017). The PM_{2.5} pollution in
 642 China has been continuously alleviating since 2013 as the implication of the Air
 643 Pollution Prevention and Control Action Plan (Zheng et al., 2018; Zhang et al., 2019),

648 especially in the Beijing-Tianjin-Hebei region (BTH) (Li et al., 2017b; Cheng et al.,
649 2019), the Yangtze River Delta (YRD) region and the Pearl River Delta (PRD) region.
650 However, severe particle pollution still occurs frequently in autumn and winter, which
651 is the major reason restricting the PM_{2.5} to come up to national standard. For example,
652 12 extremely severe and persistent PM_{2.5} pollution episodes occurred in Beijing in
653 January 2013, February 2014, December 2015, December 2016 and January 2017
654 (Zhong et al., 2018; Sun et al., 2016; Wang et al., 2018). Currently, how to effectively
655 reduce emissions in autumn and winter is the key to mitigate haze pollution in China.

656 The contribution of emission sources has been widely recognized as the decisive
657 factor of PM_{2.5} pollution over urban agglomerations, including industrial exhaust, urban
658 transportation, residential emission, power plants, agricultural activities, and bio-
659 combustion (Huang et al., 2014; Tian et al., 2016; Wu et al., 2018; An et al., 2019).
660 While the outbreak, persistence and dissipation of particle pollution generally depends
661 on the meteorological conditions and regional synoptic patterns, controlled by the large-
662 scale or synoptic-scale atmospheric circulation (Chuang et al., 2008; Zhang et al., 2012;
663 Russo et al., 2014; Zheng et al., 2015; Shu et al., 2017; Li et al., 2019).

664 Many studies have tried to reveal the relationship between synoptic patterns and
665 severe particle pollution, and estimate the meteorological contributions to these
666 pollution episodes. The YRD is mainly affected by pollutants transmitted from the
667 northern and the southern China when the East Asian major trough is located at its front
668 (Liao et al., 2017; Shu et al., 2017; Li et al., 2019). Liao et al. (2020) has confirmed that
669 the relative position of the PRD to high-pressure systems imposes significant impacts
670 on the diffusion conditions and the PM_{2.5} distributions in the PRD region. For North
671 China Plain (NCP), high frequency of stagnant weather accompanied by small pressure
672 gradient and near-surface wind speed, and shallow mixing layer are major reasons of
673 aerosol pollution over this region in winter (He et al., 2018). The aerosol pollution
674 formation process in Sichuan Basin is often controlled by the large scale high-pressure
675 circulation at sea level (Sun et al., 2020). In the Guanzhong basin, pollution event is

Deleted: d

Deleted: is

Deleted: a

generally governed by both the large-scale synoptic situation and the small-scale local circulation. The downhill wind not only forms a convergence zone in the basin, but also makes pollutants flow back from the mountain region to the basin (Bei et al., 2017). Leung et al. (2018) also find strong correlations of daily $PM_{2.5}$ variability with several synoptic patterns, including monsoon flows and cold front channels in northern China related to the Siberian High, onshore flows in eastern China, and frontal rainstorms in southern China. These previous studies have highlighted that different levels of $PM_{2.5}$ pollutions are closely related to the dominant synoptic patterns in different regions, and they attribute the large spatial variability of pollution to the regional transport contributions, not only the different local sources of $PM_{2.5}$. Thus, heavy pollution prevention and control needs to consider the weather situation, otherwise local emission reduction measures would not work well. However, under different synoptic conditions, how to effectively reduce local and regional emissions to control haze pollution is rarely reported.

Various key regions have issued the emergency preplan against the winter haze episodes, while these schemes can only be targeted at a certain city (The People's Government of Beijing Municipality, 2018; The People's Government of Shanghai Municipality, 2018) or a certain urban agglomeration (The People's Government of Guangdong Province, 2014). Although there are many studies targeted $PM_{2.5}$ mitigations at a regional scale (Ding et al., 2019; Zhang et al., 2019; Xing et al., 2018, 2019; Fu et al., 2017; etc.), their results can not be directly applied to reduce winter $PM_{2.5}$ pollution under various synoptic controls. Moreover, current emission reduction policies in China mainly aimed at sulfur dioxide (SO_2) and nitrogen dioxide (NO_2), ignoring the effective emission reduction on ammonia (NH_3), although some modeling works have discussed the effectiveness of ammonia emission reduction for $PM_{2.5}$ mitigations (Liu et al., 2019; Ye et al., 2019; Xu et al., 2019; Bai et al., 2019). Compared to remarkable reduction in SO_2 , NO_2 , and primary PM emissions, NH_3 emissions has remained stable during 2014–2018 in China (Zheng et al., 2018). In addition, given the

Deleted: T

Formatted: Font:Not Bold

Formatted: Font:Not Bold

Deleted: y always have no binding forces on the larger scale emission reduction outside of a specific region, which is not conducive to effective $PM_{2.5}$ mitigations.

Formatted: Font:Not Bold

Formatted: Subscript

Deleted: G

712 important roles of other PM_{2.5} precursors (eg., NMVOCs) in aerosol formation (Geng
 713 et al., 2019), cutting non-SO₂-NO₂-PM emissions should be proposed as a next-step
 714 mitigation strategy. Therefore, for PM_{2.5} mitigations in a specific region during winter
 715 haze episodes forced by various synoptic conditions, whether the air pollution
 716 emergency management and control schemes are effective and how to improve them
 717 have become an urgent scientific question to be answered.

718 In order to investigate the effectiveness of emission control to reduce PM_{2.5}
 719 pollution during winter haze episodes under various potential synoptic controls (PSCs),
 720 we take the severe particle pollution of winter haze episodes over Jingzhou, the
 721 hinterland of Yangtze River middle basin in Central China, as an example. Central
 722 China is geographically surrounded by major haze pollution regions, the SCB to the
 723 west, the PRD to the south, the YRD to the east, and the NCP to the north (Fig. 1). As
 724 a regional pollutant transport hub with sub basin topography, Central China is a region
 725 of transmission-pollution characteristics affected by two reported transport pathways
 726 from the vast flatland in central eastern China (Yu et al., 2020) and from the NCP region
 727 (Zheng et al., 2019a). In combination with high anthropogenic emissions (Wu et al.,
 728 2018) and secondary aerosol formation (Huang et al., 2020), Central China often suffers
 729 severe pollution episodes in winter caused by PM_{2.5} (Gong et al., 2015; Xu et al., 2017).
 730 In this study, we conduct the circulation classification to differentiate the synoptic
 731 modes during the severe particle pollution episodes in winter over Central China from
 732 2013 to 2018 by using Lamb-Jenkenson method. Then we simulate the PM_{2.5} chemical
 733 components, and the contributions of local sources as well as transboundary transport
 734 of PM_{2.5} under different synoptic conditions. Finally, the effectiveness of emission
 735 reduction in main potential synoptic patterns are evaluated by GEOS-Chem model
 736 simulations. This study combines the atmospheric (circulation classification) and
 737 environmental (chemical transport modeling) research methods and could provide
 738 reference for emission control of severe winter haze pollution under different weather
 739 types, and provide basis for regional air quality policy-making.

Deleted: NH₃
 Deleted: secondary inorganic
 Deleted: ; Liu et al., 2019
 Deleted: NH₃
 Deleted: in a specific region
 Deleted: potential
 Deleted:
 Deleted: controls
 Deleted: s

Deleted: Jingzhou

Deleted: portation

Deleted:

752
753
754
755
756
757
758
759
760
761
762
763
764
765
766
767
768
769
770
771
772
773
774
775
776
777
778
779

2 Data and Methods

2.1 Data

Hourly mass concentrations of PM_{2.5} at Jingzhou (112.18°E, 30.33°N, 33.7 m) from November 2013 to December 2018 are obtained from Hubei Environmental Monitoring Central Station (<http://sthjt.hubei.gov.cn/>). We screen the pollution days with daily mean PM_{2.5} concentrations larger than 150 µg/m³ for circulation classification.

Figure 1

We use the daily mean sea level pressure (SLP) between 2013 and 2018 from the National Centers for Environmental Prediction/National Center for Atmospheric Research (NCEP/NCAR) Final (FNL) Operational Global Analysis data (horizontal resolution: 1° × 1°; temporal resolution: 6 hours; <https://rda.ucar.edu/datasets/ds083.3/>) to conduct the classification of Lamb-Jenkenson circulation types.

The meteorological data of surface observations at Jingzhou, including ambient temperature, relative humidity, wind speed, wind direction and atmospheric pressure, are obtained from Hubei Meteorological Information and Technology Support Center (<http://hb.cma.gov.cn/qxfw/index.html>). The data from November 2013 to February 2014 are used to analyze the meteorological characteristics during the period, four severe particle pollution events occurred in succession over Central China (Fig. S1).

In order to better evaluate the GEOS-Chem model performances, we also use the PM_{2.5} observations (a total of 633 sites; from November 2013 to February 2014) from Ministry of Ecology and Environment of China (MEE, <http://www.mee.gov.cn/>) to conduct the model-observation comparison.

2.2 Lamb-Jenkenson Circulation Classification

Moved (insertion) [1]
Deleted: s

Deleted: used in this study are

Deleted: , in which

Formatted: Font color: Text 1

Formatted: Font color: Text 1

Formatted: Hyperlink, Font:Font color: Auto

Field Code Changed

Formatted: Font color: Text 1

Moved up [1]: We use the daily mean sea level pressures (SLP) from the National Centers for Environmental Prediction/National Center for Atmospheric Research (NCEP/NCAR) Final (FNL) Operational Global Analysis data (horizontal resolution: 1° × 1°; temporal resolution: 6 hours; <https://rda.ucar.edu/datasets/ds083.3/>) to conduct the classification of Lamb-Jenkenson circulation types. -

790 The atmospheric circulation classification adopts the Lamb-Jenkenson method
 791 proposed by Lamb et al. (1950) and developed by Jenkenson et al. (1977). Compared
 792 to the objective classification method PCA used in some studies (Chang and Zhan, 2017,
 793 Dai et al., 2021), this Lamb-Jenkenson method is a combination of subjective and
 794 objective methods. After the objective judgment of the circulation, we also make
 795 subjective considerations to overcome the weaknesses of their respective, leading to
 796 better synoptic significance. Many works of circulation classification have used the
 797 Lamb-Jenkenson method and reported that the analysis can well respond to the
 798 classification results (Philipp et al., 2016; Santurtun et al., 2015; Pope et al., 2015; Russo
 799 et al., 2014; Pope et al., 2014; Trigo and DaCamara, 2000).

800 To calculate the circulation types of Jingzhou, we mark total 16 points (97.5°E-
 801 127.5°E, 20°N-40°N) by every 10 longitudes and 5 latitudes and the center point
 802 located at 112.5° E and 30° N (Fig. S2). Using the sea level pressure of 16 points, we
 803 calculate six circulation indexes by scheme of central difference:

804
$$u = 0.5[P(12) + P(13) - P(4) - P(5)]$$

805 (1)

806
$$v = \frac{1}{\cos \alpha} \times \frac{1}{4} [P(4) + 2P(9) + P(13) - P(4) - 2P(8) - P(12)]$$

807 (2)

808
$$V = \sqrt{u^2 + v^2}$$

809 (3)

810
$$\xi_u = \frac{\sin \alpha}{2 \sin \alpha_1} [P(15) + P(16) - P(8) - P(9)] - \frac{\sin \alpha}{2 \sin \alpha_2} [P(8) + P(9) - P(1) - P(2)]$$

811 (4)

812
$$\xi_v = \frac{1}{8 \cos^2 \alpha} [P(6) + 2P(10) + P(14) - P(5) - 2P(9) - P(13) \\ + P(3) + 2P(7) + P(11) - P(4) - 2P(8) - P(12)]$$

813 (5)

Formatted: Font color: Text 1

Deleted: T

Formatted: Font color: Text 1

Deleted: ,

Deleted: ing

Deleted: (Trigo and DaCamara, 2000)

Deleted: leading to

Deleted: better synoptic significance (Pope et al., 2015).

Formatted: Font:Font color: R,G,B (4,50,255)

820 $\xi = \xi_u + \xi_v$

821 (6)

822 Where $P(n)(n=1,2,3\cdots 16)$ is the sea level pressure at the n^{th} point;
 823 α, α_1 and α_2 are the latitude values of points C, A_1 and A_2 , respectively; v is the
 824 geostrophic wind, u and v are the latitudinal and meridional components of the
 825 geostrophic wind; ξ is the geostrophic vorticity; ζ_u is the u meridional gradient,
 826 and ζ_v is the v latitudinal gradient.

827 Taking the latitude of the center point as the reference frame, the unit of six
 828 circulation indexes is $hPa/(10^\circ \text{lon})$, the direction of geostrophic wind can be
 829 determined by u and v , and cyclones and anticyclones can be determined by ξ .
 830 According to the geostrophic wind speed, wind direction and vorticity value, the
 831 circulation is divided into 10 types. The classification standard and corresponding types
 832 are shown in Table 1.

833

834 Table 1

835

836 2.3 GEOS-Chem simulations

837 The GEOS-Chem chemistry transport model is used
 838 (<http://acmg.seas.harvard.edu/geos/>) to simulate the spatiotemporal distribution of
 839 $\text{PM}_{2.5}$. The nested model, covering China (70°E - 140°E , 15°S - 55°N), is run with a
 840 horizontal resolution of 0.25° latitude \times 0.3125° longitude and 72 vertical layers. The
 841 boundary condition of nested model is provided by the GEOS-Chem global model with
 842 a horizontal resolution of 2° latitude \times 2.5° longitude (Fig. S3). Both global and nested
 843 simulations, driven by the GEOS-FP assimilated meteorological data, include detailed
 844 tropospheric Ozone- NO_x -VOCs- HO_x -aerosol chemistry. More details are shown in
 845 Yan et al. (2019). In the models, anthropogenic and natural sources are fully considered

Deleted: The

847 in GEOS-Chem. Table S1 and Table S2 show a list of emission inventories in the global
 848 model and nested simulation, respectively. In China, the monthly grid data of $0.25^\circ \times$
 849 0.25° from MEIC inventory (<http://meicmodel.org>) for CO, NO_x, SO₂ and non-methane
 850 volatile organic compounds (NMVOCs) in 2013-2014 is used. Over Central China,
 851 anthropogenic sources of these species are from our group SEEA (Source Emission and
 852 Environment Research) inventory with the grid data of $0.1^\circ \times 0.1^\circ$ (not shown). The
 853 SEEA emission inventory was developed based on the year of 2017 for the Wuhan city
 854 cluster and it has been successfully adopted for the air quality simulating and
 855 forecasting of 7th CISM Military World Games in 2019. Other emission descriptions
 856 are shown in Supplementary Sect. S1.

857 In order to better simulate the spatiotemporal distribution of PM_{2.5} over Central
 858 China, especially in winter heavy pollution periods, the standard v11-01 of GEOS-
 859 Chem is optimized according to the actual situation in China (see details in
 860 Supplementary Sect. S2), including optimizing PM_{2.5} sources and increasing the
 861 proportion of sulfate primary emission (Yan et al., 2020). The PM_{2.5} primary
 862 anthropogenic emissions enhance the PM_{2.5} concentrations over Central China by 5-20
 863 $\mu\text{g}/\text{m}^3$ in winter (Fig. S4). Compared with the results before the model optimization
 864 (Fig. S5), the sulfate concentration simulated by the optimized model increased from
 865 10-20 $\mu\text{g}/\text{m}^3$ to 30-50 $\mu\text{g}/\text{m}^3$. Further comparisons of PM_{2.5} with observations and
 866 inorganic salts (sulfate, nitrate and ammonium) with reported values from previous
 867 studies are shown in Sect.3.3.

869 3. Results and Discussion

870 3.1 Classification of PSCs

871 As shown in Fig. 2, among the circulation patterns of pollution-day at Jingzhou
 872 from 2013 to 2018, the frequency of SW-type circulation is the highest, accounting for
 873 29% of the total pollution days. The frequencies of NW-type, A-type and C-type are
 874 also high, accounting for 27%, 19% and 12%, respectively. While the other six

Deleted: s

Deleted: 3

Deleted: 4

Deleted: The concentration of

Formatted: Not Superscript/ Subscript

Formatted: Font color: Text 1

Deleted: increased and improved

Deleted: Potential synoptic controls (

Deleted:)

circulation patterns are less occurred, with the frequencies less than 5%. Thus, the above four typical circulation types are considered as the main potential synoptic controls of the severe particle pollution episodes over Central China.

Figure 2

3.2 Characteristics of the four main PSCs

SW-type circulation is the predominant PSC of severe PM_{2.5} pollution episodes. The circulation at 500 hPa is relatively flat and the whole East Asia region is affected by the westerly flow (Fig. S6a). Westerly belt fluctuates greatly at 700 hPa and there are two ridges and a southwest trough in the middle latitudes of Asia (Fig. S7a). Jingzhou is located in the front of a trough, prevailing the weak southwest airflow. At 850 hPa, the cold high pressure center is formed in Xinjiang of China. Warm low pressure appears in the low latitude area and weak high pressure appears in the East China Sea (Fig. 3a). In combination with the surface field, a high-low-high saddle like field forms from west to east (Fig. 4a). Such synoptic type is also the dominant weather system of eastern China (Shu et al., 2017; Yang et al., 2018). Jingzhou is located in the back of Bohai-northeast high pressure and the front of southwest warm low pressure. Thus it is affected by the southerly airflow, which could be conducive to the transport of air pollutants formed over southern China to Central China. Associated with small local surface wind speed (< 3 m/s) at Jingzhou, the dispersion of local and transported pollutants is inhibited.

Formatted: Subscript

Deleted: mainly occurs in winter (December, January and February)

Deleted: 5

Deleted: middle latitude presents

Deleted: 6

Deleted: ,

Deleted: and

Deleted: a

Figure 3

NW-type circulation mainly occurs in the early winter (December and January). This synoptic pattern is also reported as one of the main types to affect the aerosol distributions over eastern China (Zheng et al., 2015). Circulation at 500 hPa is

918 controlled by one trough and one ridge, with the weak ridge located in the northwest of
 919 China and the shallow trough located in the northeast of China (Fig. S6b). The whole
 920 East Asia is affected by the westerly current. The trough and ridge at 700 hPa are
 921 deepened. Jingzhou is located at the bottom of the shallow trough, prevailing the west-
 922 northwest airflow, affected by the flow around the plateau (Fig. S7b). At 850 hPa, the
 923 cold high pressure center is formed in Xinjiang, and Jingzhou is affected by the
 924 northerly airflow, due to being in the front of the high pressure (Fig. 3b). For the sea
 925 level pressure, the cold high pressure is located in the west of Mongolia and Xinjiang
 926 of China (Fig. 4b). Jingzhou is located at the region with weak fluctuation in the front
 927 of the high pressure, and the surface wind speed is smaller than 2 m/s. The haze episodes
 928 induced by NW-type synoptic pattern is similar to the transmission-accumulation
 929 pollution caused by SW-type, but the transmission path is from Northern China to
 930 Central China.

Figure 4

934 A-type circulation also mainly occurs in the early winter. The high-altitude
 935 circulation field is controlled by one trough and one ridge (Fig. S6c and S7c). East Asia
 936 is affected by west-northwest air flow, and the SLP is controlled by a huge high
 937 pressure, with the center located in the southwest of Baikal Lake (Fig. 4c). A surface
 938 high pressure favors accumulation of air pollutants, especially over the regions of high
 939 pressure center (Leung et al., 2018). Jingzhou is in the sparse pressure field in front of
 940 the high pressure (Fig. 3c and 4c), with an average surface wind speed of ~1.3 m/s. The
 941 uniform west-northwest air flow at high altitude would lead to the low water vapor
 942 content and less cloud amount, which is conducive to radiation cooling at night. In
 943 addition, due to the weak high pressure ridge in the north, it is not conducive to the
 944 eastward and southward movement of cold air, leading to the stable weather situation

Deleted: 5

Deleted: Affected by the flow around the plateau and the shallow trough in the northeast,

Deleted:

Deleted: 6

Deleted: (SLP) field

Deleted: 5

Deleted: 6

Deleted: s

Deleted: the

Deleted: the

Deleted: observed

Deleted: er

958 ~~and thus severe haze pollution at Jingzhou.~~ This type is also responsible for most of the
 959 severe particulate pollution days in the BTH and YRD regions (Li et al., 2019).

960 C-type circulation mainly occurs in ~~late~~ winter ~~and early~~ spring, when the relative
 961 humidity is large with ~~an~~ average value of 74%. East Asia is controlled by the straight
 962 westerly flow, and the southwest shallow trough is obvious at 500 hPa (Fig. S6d).

963 ~~Additionally,~~ the West Pacific subtropical high extends ~~s~~ to the west, Central China is
 964 affected by the southwest flow. Southwest trough is deepened at 700 hPa, and Jingzhou
 965 is located in front of the trough and controlled by the southwest airflow (Fig. S7d). High
 966 pressure ~~at~~ the south of Xinjiang and the north of Plateau is strengthened at 850 hPa,
 967 and the southwest low pressure center is formed (Fig. 3d). Jingzhou is located in the
 968 low pressure system on the SLP field (Fig. 4d), with small surface wind speed (0-3 m/s).

969 ~~Together with the large relative humidity, which can promote the hygroscopic growth~~
 970 ~~of particulate matter (Twohy et al., 2009; Zheng et al., 2015), the haze pollution is~~
 971 ~~persistent and serious at Jingzhou.~~ The impact of low-pressure systems on winter heavy
 972 air pollution have also been reported in the northwest Sichuan Basin (Ning et al., 2018).

974 3.3 PM_{2.5} and chemical components under the four main PSCs in control 975 simulations

976 The spatiotemporal distribution of PM_{2.5} and its components under the four typical
 977 synoptic controls over Central China were simulated by optimized GEOS-Chem model.
 978 ~~In order to reduce the simulation cost, the continuous four severe haze episodes~~
 979 ~~occurred during November, 2013-February, 2014 are selected. These four haze~~
 980 ~~episodes are controlled by~~ the synoptic ~~pattern~~ of SW-type (18-25 November, 2013),
 981 NW-type (19-26 December, 2013), A-type (14-21 January, 2014) and C-type (26
 982 January - 2 February, 2014), ~~respectively~~. The air quality at Jingzhou during the four
 983 pollution episodes is between grade 5 (PM_{2.5} > 150 µg/m³) and grade 6 heavy pollution
 984 (PM_{2.5} > 250 µg/m³, as Fig. 5a and S1a shown). The simulation time is started at

Deleted: .

Deleted: ,

Deleted: and autumn

Deleted: the

Deleted: 5

Deleted: In combination with

Deleted: ing

Deleted: 6

Deleted: in

Deleted:

Deleted: (Table 2)

Deleted: T

Deleted: time periods

Deleted:

Deleted: covering

Deleted: controls

Deleted: are selected

1002 November 1st, 2013, with the first two weeks used as spin up to eliminate the impact
1003 of initial conditions.

1004

1005 Figure 5

1006 Figure 6

1007

1008 The daily/hourly mean PM_{2.5} concentrations at Jingzhou in the four typical heavy
1009 pollution processes simulated by the control (CON) simulation (Table 2) are compared
1010 with the observations (Fig. 5a/Fig. S1a). The model underestimates the observed PM_{2.5}
1011 concentrations (by 43.3 µg/m³ on average), especially in the high PM_{2.5} periods (by
1012 116.8 µg/m³ at the maximum occurring in November 21-23, 2013). The possible causes
1013 for underestimation are meteorological field deviations (an overestimate in temperature
1014 and wind speed and an underestimate in humidity; Table S3) and emission errors.
1015 Anthropogenic emissions for PM_{2.5} precursors used here are for the year 2017 over
1016 Central China from SEEA inventory (Table S4). From 2013 to 2017, anthropogenic
1017 NO_x, SO₂ and primary PM_{2.5} emissions in Central China have declined substantially
1018 (Table S4), due to implementation of stringent emission control measures for the 12th-
1019 13th Five-Year Plans (Zheng et al., 2018). The anthropogenic emissions biases may
1020 affect our simulations and PM_{2.5} attribution results to some extent. Additionally, the
1021 underestimation is on a national scale when compared with the MEE observations, with
1022 a bias of -29.3 µg/m³, -18.7 µg/m³, -39.0 µg/m³ and -21.4 µg/m³ on average for SW-
1023 type, NW-type, A-type and C-type synoptic controlled episodes, respectively (Fig. 6).
1024 The national negative biases may be also attributed to insufficient resolution of the
1025 model (Yan et al., 2014), and imperfect chemical mechanisms (Yan et al., 2019).
1026 Nevertheless, the model can reproduce the evolution of each severe particle pollution
1027 episode well, including the accumulation of pollutants, the continuing process and the
1028 gradual dissipation of pollution (Fig. 5a/Fig. S1a).

1029

Formatted: Centered, Indent: First line: 0 ch

Formatted: Left, Indent: First line: 0 ch

Formatted: Font color: Text 1

Formatted: Font color: Text 1, Subscript

Formatted: Font color: Text 1

Formatted: Font color: Text 1, Superscript

Formatted: Font color: Text 1

Formatted: Font color: Text 1, Subscript

Formatted: Font color: Text 1

Formatted: Font color: Text 1

Formatted: Font color: Text 1

Deleted: The possible causes for underestimation are emission errors (Lin et al., 2016), meteorological field deviations (Liu et al., 2018)

Moved (insertion) [2]

Deleted: ,

Moved up [2]: emission errors (Lin et al., 2016), meteorological field deviations (Liu et al., 2018)

1036
1037
1038
1039
1040
1041
1042
1043
1044
1045
1046
1047
1048
1049
1050
1051
1052
1053
1054
1055
1056
1057
1058
1059
1060
1061
1062
1063

Table 2

In order to examine the model performances in the PM_{2.5} chemical compositions, we have reviewed the reported concentrations of PM_{2.5} and the three inorganic salts (sulfate, nitrate and ammonium) in other cities (Table 4). The contributions of sulfate, nitrate and ammonium are 9.1%-31.9%, 5.7%-32.1% and 5.9%-13.3%, respectively. Figure S8/S9 shows the modeled spatial distribution of PM_{2.5}, sulfate, nitrate and ammonium concentrations averaged in the four typical heavy pollution processes over Jingzhou/China. The fractions of each inorganic salt to PM_{2.5} for these four heavy pollution episodes are also shown in Fig. S10. Over Central China, the main components of PM_{2.5} are the three inorganic salts in these pollution episodes, with the averaged contributions of sulfate, nitrate and ammonium being ~20%, ~18% and ~13%, respectively (Table 3). Our modelling results are comparable to the previous observed results (Table 4). Huang et al. (2014) have also reported that the three secondary inorganic particles rank the highest fraction among the PM_{2.5} species in Central-Eastern China. As shown in Table 3, in addition to inorganic salts, other chemical components include dust (~15%), black carbon (~7%), primary organic aerosol (~14%) and second organic aerosol (~13%). In these four pollution events, the differences in mass percentages of each chemical component ranged from 0.1% (dust) to 6.2% (sulfate) (Table 3). See details in Sect. 3.4 for further analysis of the causes for the differences.

Deleted: 7
Deleted: 8
Deleted: for
Deleted: The spatial distribution of the three inorganic salts is similar to that of PM_{2.5}.

Formatted: Font color: Text 1
Deleted: Table 3

Formatted: Font color: Auto

Table 3

Table 4

3.4 Local emissions versus transmission contributions to PM_{2.5} under the four main PSCs

In order to investigate the effectiveness of emission control to reduce PM_{2.5} pollution of Central China in the four typical severe particle pollution episodes, firstly

Deleted: -
3.4 Local emissions versus tran
Deleted: sportation

we estimate the local sources versus transmission contributions of PM_{2.5} by GEOS-Chem sensitivity simulations (Table 2). Results of XJ0 (Emissions outside Jingzhou are zero) indicates the contribution of local emission sources to the PM_{2.5} pollution over Jingzhou. The difference between CON and XCC0 (Emissions outside Central China are zero) shows the transmission contribution of PM_{2.5} outside Central China to Jingzhou. The difference between CON and NCP0/YRD0/PRD0/SCB0 (Emissions over NCP/YRD/PRD/SCB are zero) represents the contribution of pollution transport from NCP/YRD/PRD/SCB regions to Jingzhou.

1081

1082

1083

For the SW-type synoptic situation, differences between the simulation results of NCP0/YRD0/SCB0 and CON show that pollution controlled by SW-type circulation over Central China is almost not affected by the emission sources from North China/East China/Sichuan Basin. The concentrations of PM_{2.5} and three inorganic salts simulated by NCP0/YRD0/SCB0 are similar to those simulated by CON, with a difference less than 3.0% (Fig. 8). However, affected by the southerly airflow at 850 hPa (Fig. 7), air pollutants formed over southern China could be transmitted to Central China, with the transport contribution of 7.6%. In addition, the contributions from transboundary transport from non-Jingzhou Central China is simulated to be 12.0% by comparing the results of XJ0 and XCC0. The transport of air pollutants from the south leads to the smallest proportion of the three inorganic salts (45.7%) in Jingzhou among the four pollution episodes (50.3%-55.5% for other three episodes), because the emissions of SO₂, NO₂ and NH₃ in the south (especially in Guangxi and Guizhou province) are smaller than those in Central China (Li et al., 2017a). Associated with the small surface wind speed of 2.1 m/s on average (Fig. 5) and the weak ascending in the vertical direction (Fig. 7) at Jingzhou, it is not conducive to the dispersion of local pollutants (Zheng et al., 2015). The high PM_{2.5} concentrations are mainly accumulated

Deleted: portation

Deleted: portation

Deleted: ation

Deleted: 6

Deleted: 7

Deleted: 6

Deleted: ation

Deleted: The transportation of air pollutants from the south makes the proportion of the three inorganic salts (45.7%) in Jingzhou area the smallest

Deleted: 6

1112 by local emissions. The simulations of XJ0 and CON show that local emission sources
1113 over Jingzhou contribute ~70% to PM_{2.5}.

1114

1115 Figure 8.

1116 Figure 9.

1117

1118 For the NW-type synoptic mode, affected by the northerly airflow (Fig. 9), it is
1119 conducive to the southward movement of air pollutants in northern China (He et al.,
1120 2018; Leung et al., 2018). Influenced by the local and surrounding terrain over Central
1121 China (Fig. 1), two ~~transmission~~ channels are formed from north to south and from
1122 northeast to southwest (Fig. 9). In addition, due to the local small wind speed (1.4 m/s
1123 on average) near the ground (Fig. 5), the weak convection and the warm ridge along
1124 the East Asia coast (Fig. 9), the local and transported pollutants accumulate in Central
1125 China. The average concentration of PM_{2.5} in Jingzhou is 179.4 µg/m³. Due to the
1126 transport contribution of pollutants from northern China (with much higher
1127 anthropogenic emissions of SO₂, NO₂ and NH₃) (Li et al., 2017a), the total proportion
1128 of the three inorganic salts is the highest (55.5%). The PM_{2.5} concentration simulated
1129 in NCP0 is 63.1% of that by CON simulation (Fig. 8), indicating that the ~~transmission~~
1130 contribution from North China in this heavy pollution episode is as high as 36.9%. The
1131 contribution of local emission sources is much smaller than that of SW-type synoptic
1132 pattern, only 41.2% (comparison between XJ0 and CON).

1133

1134 Figure 10.

1135

1136 Under the A-type circulation, Jingzhou is controlled by a high pressure system
1137 (Fig. 10) which can lead to stable weather conditions caused by radiation inversion
1138 (Guo et al., 2015) and subsidence inversion (Kurita et al., 1985), being favorable to
1139 continuous accumulation of local pollutants (Guo et al., 2015). The distribution of PM_{2.5}

Deleted: the

Formatted: Indent: First line: 14 ch

Deleted: 7 .

Deleted: 8

Deleted: 8

Deleted: trans

Deleted: portation

Deleted: 8

Deleted: 8

Deleted: ation

Deleted: 7

Deleted: portation

Deleted: the

Deleted: 9

Deleted: 9

1154 in China is similar to that of SW-type weather condition, with an averaged PM_{2.5}
1155 concentration of 128.6 µg/m³ over Central China. Unlike SW-type, the PM_{2.5} at
1156 Jingzhou in this synoptic pattern is less affected by transboundary transport, with the
1157 total transport contribution of the surrounding four major pollution regions being less
1158 than 9%. The contribution of local emission sources is about 82% (Fig. 8).

1159

1160

1161

Figure 11.

1162 Under the C-type synoptic pattern, the southwest low pressure center is formed at
1163 850 hPa, and Jingzhou is located in the low pressure system of the SLP field (Fig. 11).
1164 In combination with the large relative humidity (78% on average; Fig. 5), because that
1165 the occurrence season of C-type is the late winter and early spring, it can promote the
1166 haze pollution due to its impact on hydrophilic aerosols (Twohy et al., 2009; Zheng et
1167 al., 2015). Together with the small wind speed (less than 4 m/s; Fig. 5), it is easy to
1168 cause the accumulation of pollutants. The average concentration of PM_{2.5} over Central
1169 China is as high as 203.7 µg/m³. Air pollution controlled by this weather condition is
1170 the most serious of the four typical synoptic controls. However, in this weather situation,
1171 pollutants in North China are easy to diffuse (Miao et al., 2017; Li et al., 2019), and the
1172 concentration of PM_{2.5} is significantly lower than that in the former three weather
1173 situations (Fig. 11 and Fig. S9). The contribution of pollution transport from non-
1174 Central China region simulated by GEOS-Chem is less than 8%, and the contribution
1175 of local emission sources at Jingzhou is more than 85% (Fig. 7).

1176

1177 3.5 Effectiveness of emission reduction under the four main PSCs

1178 In order to estimate the effectiveness of emission reduction in severe pollution
1179 events forced by the four potential synoptic controls, we conduct sensitivity simulations
1180 by applying seven emission scenarios (Table 2). All emission scenarios use the
1181 reduction ratio of 20% which is close to the average of the target emission reduction of

Deleted: ation

Deleted: 7

Deleted: 0

Deleted: on

Deleted: 0

Deleted:)

Deleted: owing

Deleted: 0

Deleted: 8

all provinces in the 13th Five-year plan (The State Council of the People's Republic of China, 2016). Although the base year of emission reduction is 2015 for the 13th Five-year plan, it does not affect to use the simulation results of emission scenarios (with the reduction ratio of 20% applied to the simulated year 2013/2014) to explore the emission reduction effect of specific haze pollution events. The differences in model results between CON (control simulation) and JSN/JSNN/JALL (emissions of SO₂+NO_x/SO₂+NO_x+NH₃/all pollution sources at Jingzhou are reduced by 20%) represent the environmental benefits caused by different local emission reduction scenarios. The potential PM_{2.5} mitigations by joint prevention and control in different regions are calculated by sensitivity experiments of CCALL (emissions of all pollution sources over Central China are reduced by 20%), CNALL (over Central China and NCP region), CPALL (over Central China and PRD region) and TALL (over Central China, NCP, YRD, PRD and SCB regions).

In the JSN emission reduction scenario, the sulfate and ammonium concentrations over Jingzhou are significantly reduced by 3.2-5.8 µg/m³ (12.7-14.5%) and 0.6-1.9 µg/m³ (3.2-5.9%) in these four pollution events, respectively. However, the concentration of nitrate increases (1.3-1.7%). This is because there is a competition mechanism between nitrate and sulfate. Ammonium ions always react with sulfate ions first to generate ammonium sulfate, which will continue to react with nitrate ions to generate ammonium nitrate when ammonium ions are rich (Mao et al., 2010). Thus the reduction of SO₂ emission increases the concentration of nitrate, which offset the contribution of sulfate particle reduction to the environment to some extent. Therefore, the application of JSN emission reduction scheme only reduces the PM_{2.5} concentrations by 3.1-7.2 µg/m³ (2.0-3.5%, Fig. 12). This inefficient emission reduction scheme is most widely used in heavy pollution areas over China in the past decade, ignoring the synergistic effect of various precursors.

Figure 12

Formatted: Superscript

Formatted: Subscript

Deleted: The modeling results indicate that there are enough NH₃ emissions over Central China to consume all sulfate ions, but not enough to combine with all nitrate ions.

Deleted: 1

Deleted: 1

1224

1225 By applying the JSNN and JALL emission reduction scenarios, we aim to evaluate
1226 the synergistic effect of multiple precursors on emission reduction. These two scenarios
1227 reduce the average sulfate concentration in Jingzhou by 2.8-6.7 $\mu\text{g}/\text{m}^3$ (11.3-17.3%)
1228 and 2.9-7.2 $\mu\text{g}/\text{m}^3$ (11.7-17.9%), and the ammonium concentration by 2.0-4.8 $\mu\text{g}/\text{m}^3$
1229 (12.1-16.5%) and 2.2-4.7 $\mu\text{g}/\text{m}^3$ (13.2-17.3%), respectively. Unlike the increments of
1230 nitrate in JSN emission reduction scenario, the nitrate decreases (JSNN: 0.3-1.2 $\mu\text{g}/\text{m}^3$;
1231 JALL: 0.4-1.5 $\mu\text{g}/\text{m}^3$). Therefore, through the application of JSNN and JALL emission
1232 reduction schemes, $\text{PM}_{2.5}$ concentrations decrease by 4.9-8.3% and 9.0-15.9%,
1233 respectively (Fig. 12), much higher than the improvement by JSN scenario. Zheng et
1234 al. (2019b) has also evaluated the sensitiveness of NH_3 control to $\text{PM}_{2.5}$ reduction based
1235 on observations. However, these results indicate that it is unrealistic to substantially
1236 reduce local emissions to achieve the national air quality standard in the long term.

1237 Additionally, the sensitivity simulations by excluding emission sources over
1238 upwind regions are conducted to estimate the potential $\text{PM}_{2.5}$ mitigations of inter-
1239 regional and intra-regional joint control. Our results show that after applying TALL
1240 emission reduction scenario, $\text{PM}_{2.5}$ concentrations have been significantly improved,
1241 with the improvement rates increased from 9.0-15.9% (by JALL scenario) to 17.4-18.8%
1242 (Fig. 12). Especially, the NW-type synoptic controlled air pollution episode shows the
1243 best effect of joint prevention, followed by SW-type. For NW-type, by reducing
1244 emissions over Central China and Northern China (CNALL scheme), $\text{PM}_{2.5}$
1245 concentrations are reduced by 26.5 $\mu\text{g}/\text{m}^3$ (16.9%), much more effective than JALL
1246 emission reduction scheme (14.1 $\mu\text{g}/\text{m}^3$, 9.0%). In SW-type controlled pollution
1247 episode, it should be otherwise to decrease the emissions over Southern China in
1248 addition to Central China.

1249

1250 4. Conclusion

Deleted: 1

Deleted: 1

1253 The PM_{2.5} pollution in autumn and winter haze periods is now the key obstacle for
 1254 further improving air quality in China. The extremely severe and persistent PM_{2.5}
 1255 pollution episodes are attributed to adverse synoptic conditions in addition to high
 1256 precursor emissions. For the PM_{2.5} mitigations during winter haze episodes in specific
 1257 region forced by various potential synoptic controls, how to effectively reduce
 1258 emissions has become an urgent scientific question to be answered. Our results over
 1259 Central China could provide reference for regional air quality policy-making.

Deleted: the

Deleted: dominant

1260 Through Lamb-Jenkenson circulation classification, the top four potential
 1261 synoptic controls of heavy PM_{2.5} pollution days (totally 109 days) over Central China
 1262 from 2013 to 2018 are decomposed to be SW-type, NW-type A-type and C-type,
 1263 accounting for 29%, 27%, 19% and 12% of the total pollution days, respectively. In
 1264 these four PSCs, three inorganic salt aerosols (sulfate: ~20%; nitrate: ~18%;
 1265 ammonium: ~13%) totally accounted for ~51% of PM_{2.5} concentrations simulated by
 1266 optimized GEOS-Chem modelling.

Deleted: (PSC)

Deleted: The difference of PM_{2.5} concentrations for the four PSC is mainly contributed by the differences of the three inorganic salts.

1267 In the SW-type/NW-type synoptic situation, affected by the southerly/northerly
 1268 airflow, pollutants over southern/northern China could be transmitted to Central China,
 1269 with the transport contribution of 7.6%/37%. In the situation A-type/C-type weather,
 1270 affected by stable weather condition/high relative humidity, the pollution processes are
 1271 less affected by the emission sources from non-local regions. And the local emission
 1272 sources dominate the contribution (82%/85%) to PM_{2.5}.

Deleted: ation

Formatted: Subscript

Deleted: contribute 82%/85% of PM_{2.5}

1273 By only reducing SO₂ and NO_x emission and not controlling NH₃, due to the
 1274 competition mechanism between nitrate and sulfate, the concentrations of sulfate and
 1275 ammonium decrease, but the concentration of nitrate increases instead. The enhanced
 1276 nitrate counteracts the effect of sulfate reduction on PM_{2.5} mitigation_s, with less than 4%
 1277 decrease in PM_{2.5}. Even if the NH₃ emission is also reduced, the PM_{2.5} concentration
 1278 reduction is less than 9%. By applying the TALL emission reduction scenario, PM_{2.5}
 1279 concentrations would decrease significantly, with the improvement rate increased from
 1280 9.0-15.9% (by JALL scenario) to 17.4-18.8%.

These results provide an opportunity to effectively mitigate haze pollution by local emission control actions in coordination with regional collaborative actions according to different synoptic patterns. Especially, the NW-type synoptic controlled air pollution episode shows the best effect of joint prevention, followed by SW-type. It is noted that in this study, the division of transmission areas is relatively rough, and more accurate source area identification and refined assessment of emission reduction effect of multiple pollutants from source groups are needed in the follow-up.

Acknowledgement

This study was financially supported by the National Natural Science Foundation of China (41830965; 41775115; 41905112), the Key Program of Ministry of Science and Technology of the People's Republic of China (2017YFC0212602; 2016YFA0602002), the Key Program for Technical Innovation of Hubei Province (2017ACA089), the Program for Environmental Protection in Hubei Province (2017HB11) and the China Postdoctoral Science Foundation funded project (258572).

Deleted: and

The research was also funded by the Fundamental Research Funds for the Central Universities, China University of Geosciences (Wuhan) (G1323519230; 201616; 26420180020; CUG190609) and the Start-up Foundation for Advanced Talents (162301182756).

Author contributions

Yingying Yan and Shaofei Kong conceived and designed the research. Yingying Yan performed the data processing, model simulations, and analyses. Yue Zhou assisted in the circulation classification. Jian Wu provided the emission data over Central China. Shaofei Kong, Tianliang Zhao and Dantong Liu contributed the funding acquisition. Yingying Yan wrote the paper with input from all authors.

Data availability

1318 Observational data are obtained from individual sources (see links in the text).
1319 Model results are available upon request. Model codes are available on a collaborative
1320 basis.

1321

1322 **Competing interests**

1323 The authors declare that they have no conflict of interest.

1324

1325 **References**

1326 The People's Government of Beijing Municipality (PGBM): Emergency plan for severe
1327 air pollution in Beijing, available at:
1328 http://www.beijing.gov.cn/zhengce/zhengcefagui/201905/t20190522_61613.html
1329 (last access: 14 July 2018), 2018 (in Chinese).

1330 The People's Government of Guangdong Province (PGGP): Emergency plan for severe
1331 air pollution in Pearl River Delta, available at:
1332 http://www.gd.gov.cn/gkmlpt/content/0/142/post_142657.html#7 (last access: 14
1333 July 2018), 2014 (in Chinese).

1334 The People's Government of Shanghai Municipality (PGSM): Special emergency plan
1335 for heavy air pollution in Shanghai, available at:
1336 <http://www.shanghai.gov.cn/nw2/nw2314/nw2319/nw31973/nw32019/nw32022/nw32023/u21aw1316153.html> (last access: 14 July 2018), 2018 (in Chinese).

1338 The State Council of the People's Republic of China (SCPPC): The Thirteenth Five-
1339 Year Plan for Energy Saving and Emission Reduction, available at:
1340 http://www.gov.cn/gongbao/content/2017/content_5163448.htm (last access: 14
1341 July 2018), 2016 (in Chinese).

1342 The State Council of the People's Republic of China (SCPPC): Air Pollution Prevention
1343 and Control Action Plan, available at: http://www.gov.cn/zhengce/content/2013-09/13/content_4561.htm (last access: 14 July 2018), 2013 (in Chinese).

1345 Jenkinson A. F., Collison F. P.: An initial climatology of gales over the North Sea.
1346 Synoptic Climatology Branch Memorandum, 62. Bracknell: Meteorological Office,
1347 1-18, 1977.

1348 Lamb H H. Types and spells of weather around the year in the British Isles. Quarterly
1349 Journal Royal Meteorological Society, 76, 393-438, 1950.

1350 Agarwal, N. K., Sharma, P., and Agarwal, S. K.: Particulate matter air pollution and
1351 cardiovascular disease, Medical Science, 21, 270-279, 2017.

Formatted: Line spacing: multiple 1.15 li

1352 An, Z., Huang, R.J., Zhang, R., Tie, X., Li, G., Cao, J., Zhou, W., Shi, Z., Han, Y., Gu,
1353 Z., and Ji, Y.: Severe haze in northern China: A synergy of anthropogenic emissions
1354 and atmospheric processes, *Proceedings of the National Academy of Sciences of the*
1355 *United States of America*, 116, 8657-8666, 10.1073/pnas.1900125116, 2019.

1356 Bei, N., Zhao, L., Xiao, B., Meng, N., and Feng, T.: Impacts of local circulations on the
1357 wintertime air pollution in the Guanzhong Basin, China, *Science of the Total*
1358 *Environment*, 592, 373-390, 10.1016/j.scitotenv.2017.02.151, 2017.

1359 Bi, X., Dai, Q., Wu, J., Zhang, Q., Zhang, W., Luo, R., Cheng, Y., Zhang, J., Wang, L.,
1360 Yu, Z., Zhang, Y., Tian, Y., and Feng, Y.: Characteristics of the main primary source
1361 profiles of particulate matter across China from 1987 to 2017, *Atmospheric*
1362 *Chemistry and Physics*, 19, 3223-3243, 10.5194/acp-19-3223-2019, 2019.

1363 Cheng, J., Su, J., Cui, T., Li, X., Dong, X., Sun, F., Yang, Y., Tong, D., Zheng, Y., Li,
1364 Y., Li, J., Zhang, Q., and He, K.: Dominant role of emission reduction in PM_{2.5} air
1365 quality improvement in Beijing during 2013-2017: a model-based decomposition
1366 analysis, *Atmospheric Chemistry and Physics*, 19, 6125-6146, 10.5194/acp-19-
1367 6125-2019, 2019.

1368 Cheng, Z., Luo, L., Wang, S., Wang, Y., Sharma, S., Shimadera, H., Wang, X., Bressi,
1369 M., de Miranda, R. M., Jiang, J., Zhou, W., Fajardo, O., Yan, N., and Hao, J.: Status
1370 and characteristics of ambient PM_{2.5} pollution in global megacities, *Environment*
1371 *International*, 89-90, 212-221, 10.1016/j.envint.2016.02.003, 2016.

1372 Chuang, M.T., Chiang, P.C., Chan, C.C., Wang, C.F., Chang, E. E., and Lee, C.T.: The
1373 effects of synoptical weather pattern and complex terrain on the formation of aerosol
1374 events in the Greater Taipei area, *Science of the Total Environment*, 399, 128-146,
1375 10.1016/j.scitotenv.2008.01.051, 2008.

1376 Geng, G., Xiao, Q., Zheng, Y., Tong, D., Zhang, Y., Zhang, X., Zhang, Q., He, K., and
1377 Liu, Y.: Impact of China's Air Pollution Prevention and Control Action Plan on PM_{2.5}
1378 chemical composition over eastern China, *Science China-Earth Sciences*, 62, 1872-
1379 1884, 10.1007/s11430-018-9353-x, 2019.

1380 Gong, W., Zhang, T., Zhu, Z., Ma, Y., Ma, X., and Wang, W.: Characteristics of PM_{1.0},
1381 PM_{2.5}, and PM₁₀, and Their Relation to Black Carbon in Wuhan, Central China,
1382 *Atmosphere*, 6, 1377-1387, 10.3390/atmos6091377, 2015.

1383 Guo, L., Guo, X., Fang, C., and Zhu, S.: Observation analysis on characteristics of
1384 formation, evolution and transition of a long-lasting severe fog and haze episode in
1385 North China, *Science China-Earth Sciences*, 58, 329-344, 10.1007/s11430-014-
1386 4924-2, 2015.

1387 He, J., Gong, S., Zhou, C., Lu, S., Wu, L., Chen, Y., Yu, Y., Zhao, S., Yu, L., and Yin,
1388 C.: Analyses of winter circulation types and their impacts on haze pollution in

Beijing, *Atmospheric Environment*, 192, 94-103, 10.1016/j.atmosenv.2018.08.060, 2018.

Huang, R.J., Zhang, Y., Bozzetti, C., Ho, K.F., Cao, J.J., Han, Y., Daellenbach, K. R., Slowik, J. G., Platt, S. M., Canonaco, F., Zotter, P., Wolf, R., Pieber, S. M., Bruns, E. A., Crippa, M., Ciarelli, G., Piazzalunga, A., Schwikowski, M., Abbaszade, G., Schnelle-Kreis, J., Zimmermann, R., An, Z., Szidat, S., Baltensperger, U., El Haddad, I., and Prevot, A. S. H.: High secondary aerosol contribution to particulate pollution during haze events in China, *Nature*, 514, 218-222, 10.1038/nature13774, 2014.

Huang, X., Ding, A., Gao, J., Zheng, B., Zhou, D., Qi, X., Tang, R., Wang, J., Ren, C., Nie, W., Chi, X., Xu, Z., Chen, L., Li, Y., Che, F., Pang, N., Wang, H., Tong, D., Qin, W., Cheng, W., Liu, W., Fu, Q., Liu, B., Chai, F., Davis, S. J., Zhang, Q., and He, K.: Enhanced secondary pollution offset reduction of primary emissions during COVID-19 lockdown in China, *National Science Review*, 10.1093/nsr/nwaa137, 2020.

Kurita, H., Sasaki, K., Muroga, H., Ueda, H., and Wakamatsu, S.: Long-range transport of air pollution under light gradient wind conditions, *Journal of Climate and Applied Meteorology*, 24, 425-434, 10.1175/1520-0450(1985)024<0425:lrtoap>2.0.co;2, 1985.

Leung, D. M., Tai, A. P. K., Mickley, L. J., Moch, J. M., van Donkelaar, A., Shen, L., and Martin, R. V.: Synoptic meteorological modes of variability for fine particulate matter (PM_{2.5}) air quality in major metropolitan regions of China, *Atmospheric Chemistry and Physics*, 18, 6733-6748, 10.5194/acp-18-6733-2018, 2018.

Li, J., Liao, H., Hu, J., and Li, N.: Severe particulate pollution days in China during 2013-2018 and the associated typical weather patterns in Beijing-Tianjin-Hebei and the Yangtze River Delta regions, *Environmental Pollution*, 248, 74-81, 10.1016/j.envpol.2019.01.124, 2019.

Li, M., Zhang, Q., Kurokawa, J.-i., Woo, J.-H., He, K., Lu, Z., Ohara, T., Song, Y., Streets, D. G., Carmichael, G. R., Cheng, Y., Hong, C., Huo, H., Jiang, X., Kang, S., Liu, F., Su, H., and Zheng, B.: MIX: a mosaic Asian anthropogenic emission inventory under the international collaboration framework of the MICS-Asia and HTAP, *Atmospheric Chemistry and Physics*, 17, 935-963, 10.5194/acp-17-935-2017, 2017a.

Li, X., Zhang, Q., Zhang, Y., Zhang, L., Wang, Y., Zhang, Q., Li, M., Zheng, Y., Geng, G., Wallington, T. J., Han, W., Shen, W., and He, K.: Attribution of PM_{2.5} exposure in Beijing-Tianjin-Hebei region to emissions: implication to control strategies, *Science Bulletin*, 62, 957-964, 10.1016/j.scib.2017.06.005, 2017b.

1426 Li, Z., Guo, J., Ding, A., Liao, H., Liu, J., Sun, Y., Wang, T., Xue, H., Zhang, H., and
 1427 Zhu, B.: Aerosol and boundary-layer interactions and impact on air quality, *National*
 1428 *Science Review*, 4, 810-833, 10.1093/nsr/nwx117, 2017c.

1429 Liao, Z., Gao, M., Sun, J., and Fan, S.: The impact of synoptic circulation on air quality
 1430 and pollution-related human health in the Yangtze River Delta region, *Science of the*
 1431 *Total Environment*, 607, 838-846, 10.1016/j.scitotenv.2017.07.031, 2017.

1432 Liao, Z., Xie, J., Fang, X., Wang, Y., Zhang, Y., Xu, X., and Fan, S.: Modulation of
 1433 synoptic circulation to dry season PM_{2.5} pollution over the Pearl River Delta region:
 1434 An investigation based on self-organizing maps, *Atmospheric Environment*, 230,
 1435 10.1016/j.atmosenv.2020.117482, 2020.

1436 Lin, Y., Zou, J., Yang, W., and Li, C.Q.: A Review of Recent Advances in Research on
 1437 PM_{2.5} in China, *International Journal of Environmental Research and Public Health*,
 1438 15, 10.3390/ijerph15030438, 2018.

1439 Liu, M., Huang, X., Song, Y., Tang, J., Cao, J., Zhang, X., Zhang, Q., Wang, S., Xu,
 1440 T., Kang, L., Cai, X., Zhang, H., Yang, F., Wang, H., Yu, J. Z., Lau, A. K. H., He,
 1441 L., Huang, X., Duan, L., Ding, A., Xue, L., Gao, J., Liu, B., and Zhu, T.: Ammonia
 1442 emission control in China would mitigate haze pollution and nitrogen deposition, but
 1443 worsen acid rain, *Proceedings of the National Academy of Sciences of the United*
 1444 *States of America*, 116, 7760-7765, 10.1073/pnas.1814880116, 2019.

1445 Mao, J., Jacob, D. J., Evans, M. J., Olson, J. R., Ren, X., Brune, W. H., Clair, J. M. S.,
 1446 Crounse, J. D., Spencer, K. M., Beaver, M. R., Wennberg, P. O., Cubison, M. J.,
 1447 Jimenez, J. L., Fried, A., Weibring, P., Walega, J. G., Hall, S. R., Weinheimer, A. J.,
 1448 Cohen, R. C., Chen, G., Crawford, J. H., McNaughton, C., Clarke, A. D., Jaeglé, L.,
 1449 Fisher, J. A., Yantosca, R. M., Le Sager, P., and Carouge, C.: Chemistry of hydrogen
 1450 oxide radicals (HOx) in the Arctic troposphere in spring, *Atmospheric Chemistry*
 1451 *and Physics*, 10, 5823-5838, 10.5194/acp-10-5823-2010, 2010.

1452 Miao, Y., Guo, J., Liu, S., Liu, H., Li, Z., Zhang, W., and Zhai, P.: Classification of
 1453 summertime synoptic patterns in Beijing and their associations with boundary layer
 1454 structure affecting aerosol pollution, *Atmospheric Chemistry and Physics*, 17, 3097-
 1455 3110, 10.5194/acp-17-3097-2017, 2017.

1456 Ning, G., Wang, S., Yim, S. H. L., Li, J., Hu, Y., Shang, Z., Wang, J., and Wang, J.:
 1457 Impact of low-pressure systems on winter heavy air pollution in the northwest
 1458 Sichuan Basin, China, *Atmospheric Chemistry and Physics*, 18, 13601-13615,
 1459 10.5194/acp-18-13601-2018, 2018.

1460 Pope, R. J., Savage, N. H., Chipperfield, M. P., Ordonez, C., and Neal, L. S.: The
 1461 influence of synoptic weather regimes on UK air quality: regional model studies of

Deleted: Lin, J., Tong, D., Davis, S., Ni, R., Tan, X., Pan, D., Zhao, H., Lu, Z., Streets, D., Feng, T., Zhang, Q., Yan, Y., Hu, Y., Li, J., Liu, Z., Jiang, X., Geng, G., He, K., Huang, Y., and Guan, D.: Global climate forcing of aerosols embodied in international trade, *Nature Geoscience*, 9, 790-+, 10.1038/ngeo2798, 2016. .

Deleted: Liu, M., Lin, J., Wang, Y., Sun, Y., Zheng, B., Shao, J., Chen, L., Zheng, Y., Chen, J., Fu, T.-M., Yan, Y., Zhang, Q., and Wu, Z.: Spatiotemporal variability of NO₂ and PM_{2.5} over Eastern China: observational and model analyses with a novel statistical method, *Atmospheric Chemistry and Physics*, 18, 12933-12952, 10.5194/acp-18-12933-2018, 2018. .

1475 tropospheric column NO₂, *Atmospheric Chemistry and Physics*, 15, 11201-11215,
1476 10.5194/acp-15-11201-2015, 2015.

1477 Russo, A., Trigo, R. M., Martins, H., and Mendes, M. T.: NO₂, PM₁₀ and O₃ urban
1478 concentrations and its association with circulation weather types in Portugal,
1479 *Atmospheric Environment*, 89, 768-785, 10.1016/j.atmosenv.2014.02.010, 2014.

1480 Shu, L., Xie, M., Gao, D., Wang, T., Fang, D., Liu, Q., Huang, A., and Peng, L.:
1481 Regional severe particle pollution and its association with synoptic weather patterns
1482 in the Yangtze River Delta region, China, *Atmospheric Chemistry and Physics*, 17,
1483 12871-12891, 10.5194/acp-17-12871-2017, 2017.

1484 Sun, Y., Niu, T., He, J., Ma, Z., Liu, P., Xiao, D., Hu, J., Yang, J., and Yan, X.:
1485 Classification of circulation patterns during the formation and dissipation of
1486 continuous pollution weather over the Sichuan Basin, China, *Atmospheric*
1487 *Environment*, 223, 10.1016/j.atmosenv.2019.117244, 2020.

1488 Sun, Y. L., Chen, C., Zhang, Y. J., Xu, W. Q., Zhou, L. B., Cheng, X. L., Zheng, H. T.,
1489 Ji, D. S., Li, J., Tang, X., Fu, P. Q., and Wang, Z. F.: Rapid formation and evolution
1490 of an extreme haze episode in Northern China during winter 2015, *Scientific Reports*,
1491 6, 10.1038/srep27151, 2016.

1492 Tian, S. L., Pan, Y. P., and Wang, Y. S.: Size-resolved source apportionment of
1493 particulate matter in urban Beijing during haze and non-haze episodes, *Atmospheric*
1494 *Chemistry and Physics*, 16, 1-19, 10.5194/acp-16-1-2016, 2016.

1495 Trigo, R. M., and DaCamara, C. C.: Circulation weather types and their influence on
1496 the precipitation regime in Portugal, *International Journal of Climatology*, 20, 1559-
1497 1581, 10.1002/1097-0088(20001115)20:13<1559::aid-joc555>3.0.co;2-5, 2000.

1498 Twohy, C. H., Coakley, J. A., Jr., and Tahnk, W. R.: Effect of changes in relative
1499 humidity on aerosol scattering near clouds, *Journal of Geophysical Research-*
1500 *Atmospheres*, 114, 10.1029/2008jd010991, 2009.

1501 Wang, X., Wei, W., Cheng, S., Li, J., Zhang, H., and Lv, Z.: Characteristics and
1502 classification of PM_{2.5} pollution episodes in Beijing from 2013 to 2015, *Science of*
1503 *the Total Environment*, 612, 170-179, 10.1016/j.scitotenv.2017.08.206, 2018.

1504 Wang, Y., Chen, Y., Wu, Z., Shang, D., Bian, Y., Du, Z., Schmitt, S. H., Su, R.,
1505 Gkatzelis, G. I., Schlag, P., Hohaus, T., Voliotis, A., Lu, K., Zen, L., Zhao, C.,
1506 Alfarra, M. R., McFiggans, G., Wiedensohler, A., Kiendler-Scharr, A., Zhang, Y.,
1507 and Hu, M.: Mutual promotion between aerosol particle liquid water and particulate
1508 nitrate enhancement leads to severe nitrate-dominated particulate matter pollution
1509 and low visibility, *Atmospheric Chemistry and Physics*, 20, 2161-2175, 10.5194/acp-
1510 20-2161-2020, 2020.

- 1511 Wu, J., Kong, S., Wu, F., Cheng, Y., Zheng, S., Yan, Q., Zheng, H., Yang, G., Zheng,
1512 M., Liu, D., Zhao, D., and Qi, S.: Estimating the open biomass burning emissions in
1513 central and eastern China from 2003 to 2015 based on satellite observation,
1514 Atmospheric Chemistry and Physics, 18, 11623-11646, 10.5194/acp-18-11623-
1515 2018, 2018.
- 1516 Xu, G., Jiao, L., Zhang, B., Zhao, S., Yuan, M., Gu, Y., Liu, J., and Tang, X.: Spatial
1517 and temporal variability of the PM_{2.5}/PM₁₀ ratio in Wuhan, Central China, Aerosol
1518 and Air Quality Research, 17, 741-751, 10.4209/aaqr.2016.09.0406, 2017.
- 1519 Yan, Q., Kong, S., Yan, Y., Liu, H., Wang, W., Chen, K., Yin, Y., Zheng, H., Wu, J.,
1520 Yao, L., Zeng, X., Cheng, Y., Zheng, S., Wu, F., Niu, Z., Zhang, Y., Zheng, M.,
1521 Zhao, D., Liu, D., and Qi, S.: Emission and simulation of primary fine and submicron
1522 particles and water-soluble ions from domestic coal combustion in China,
1523 Atmospheric Environment, 224, 10.1016/j.atmosenv.2020.117308, 2020.
- 1524 Yan, Y., Cabrera-Perez, D., Lin, J., Pozzer, A., Hu, L., Millet, D. B., Porter, W. C., and
1525 Lelieveld, J.: Global tropospheric effects of aromatic chemistry with the SAPRC-11
1526 mechanism implemented in GEOS-Chem version 9-02, Geoscientific Model
1527 Development, 12, 111-130, 10.5194/gmd-12-111-2019, 2019.
- 1528 Yan, Y. Y., Lin, J. T., Kuang, Y., Yang, D., and Zhang, L.: Tropospheric carbon
1529 monoxide over the Pacific during HIPPO: two-way coupled simulation of GEOS-
1530 Chem and its multiple nested models, Atmospheric Chemistry and Physics, 14,
1531 12649-12663, 10.5194/acp-14-12649-2014, 2014.
- 1532 Yang, Y., Zheng, X., Gao, Z., Wang, H., Wang, T., Li, Y., Lau, G. N. C., and Yim, S.
1533 H. L.: Long-term trends of persistent synoptic circulation events in planetary
1534 boundary layer and their relationships with haze pollution in winter half year over
1535 Eastern China, Journal of Geophysical Research-Atmospheres, 123, 10991-11007,
1536 10.1029/2018jd028982, 2018.
- 1537 Yu, C., Zhao, T., Bai, Y., Zhang, L., Kong, S., Yu, X., He, J., Cui, C., Yang, J., You,
1538 Y., Ma, G., Wu, M., and Chang, J.: Heavy air pollution with a unique "non-stagnant"
1539 atmospheric boundary layer in the Yangtze River middle basin aggravated by
1540 regional transport of PM_{2.5} over China, Atmospheric Chemistry and Physics, 20,
1541 7217-7230, 10.5194/acp-20-7217-2020, 2020.
- 1542 Zhang, J. P., Zhu, T., Zhang, Q. H., Li, C. C., Shu, H. L., Ying, Y., Dai, Z. P., Wang,
1543 X., Liu, X. Y., Liang, A. M., Shen, H. X., and Yi, B. Q.: The impact of circulation
1544 patterns on regional transport pathways and air quality over Beijing and its
1545 surroundings, Atmospheric Chemistry and Physics, 12, 5031-5053, 10.5194/acp-12-
1546 5031-2012, 2012.

- Zhang, Q., Jiang, X., Tong, D., Davis, S. J., Zhao, H., Geng, G., Feng, T., Zheng, B., Lu, Z., Streets, D. G., Ni, R., Brauer, M., van Donkelaar, A., Martin, R. V., Huo, H., Liu, Z., Pan, D., Kan, H., Yan, Y., Lin, J., He, K., and Guan, D.: Transboundary health impacts of transported global air pollution and international trade, *Nature*, 543, 10.1038/nature21712, 2017.
- Zhang, Q., Zheng, Y., Tong, D., Shao, M., Wang, S., Zhang, Y., Xu, X., Wang, J., He, H., Liu, W., Ding, Y., Lei, Y., Li, J., Wang, Z., Zhang, X., Wang, Y., Cheng, J., Liu, Y., Shi, Q., Yan, L., Geng, G., Hong, C., Li, M., Liu, F., Zheng, B., Cao, J., Ding, A., Gao, J., Fu, Q., Huo, J., Liu, B., Liu, Z., Yang, F., He, K., and Hao, J.: Drivers of improved PM_{2.5} air quality in China from 2013 to 2017, *Proceedings of the National Academy of Sciences of the United States of America*, 116, 24463-24469, 10.1073/pnas.1907956116, 2019.
- Zheng, B., Tong, D., Li, M., Liu, F., Hong, C., Geng, G., Li, H., Li, X., Peng, L., Qi, J., Yan, L., Zhang, Y., Zhao, H., Zheng, Y., He, K., and Zhang, Q.: Trends in China's anthropogenic emissions since 2010 as the consequence of clean air actions, *Atmospheric Chemistry and Physics*, 18, 14095-14111, 10.5194/acp-18-14095-2018, 2018.
- Zheng, H., Kong, S., Wu, F., Cheng, Y., Niu, Z., Zheng, S., Yang, G., Yao, L., Yan, Q., Wu, J., Zheng, M., Chen, N., Xu, K., Yan, Y., Liu, D., Zhao, D., Zhao, T., Bai, Y., Li, S., and Qi, S.: Intra-regional transport of black carbon between the south edge of the North China Plain and central China during winter haze episodes, *Atmospheric Chemistry and Physics*, 19, 4499-4516, 10.5194/acp-19-4499-2019, 2019a.
- Zheng, M., Wang, Y., Bao, J., Yuan, L., Zheng, H., Yan, Y., Liu, D., Xie, M., and Kong, S.: Initial Cost Barrier of Ammonia Control in Central China, *Geophysical Research Letters*, 46, 14175-14184, 10.1029/2019gl084351, 2019b.
- Zheng, X. Y., Fu, Y. F., Yang, Y. J., and Liu, G. S.: Impact of atmospheric circulations on aerosol distributions in autumn over eastern China: observational evidence, *Atmospheric Chemistry and Physics*, 15, 12115-12138, 10.5194/acp-15-12115-2015, 2015.
- Zhong, J., Zhang, X., Dong, Y., Wang, Y., Liu, C., Wang, J., Zhang, Y., and Che, H.: Feedback effects of boundary-layer meteorological factors on cumulative explosive growth of PM_{2.5} during winter heavy pollution episodes in Beijing from 2013 to 2016, *Atmospheric Chemistry and Physics*, 18, 247-258, 10.5194/acp-18-247-2018, 2018.
- Bai, Z., Winiwarter, W., Klimont, Z., Velthof, G., Misselbrook, T., Zhao, Z., Jin, X., Oenema, O., Hu, C., and Ma, L.: Further Improvement of Air Quality in China Needs

Formatted: Font:(Default) Times New Roman, 12 pt, Font color: Auto

Formatted: EndNote Bibliography, Indent: Left: 0 cm, Hanging: 1 ch, First line: -1 ch, Don't add space between paragraphs of the same style, Line spacing: multiple 1.15 li

[Clear Ammonia Mitigation Target, Environmental Science & Technology, 53, 10542-10544, 10.1021/acs.est.9b04725, 2019.](#)
[Xu, Z., Liu, M., Zhang, M., Song, Y., Wang, S., Zhang, L., Xu, T., Wang, T., Yan, C., Zhou, T., Sun, Y., Pan, Y., Hu, M., Zheng, M., and Zhu, T.: High efficiency of livestock ammonia emission controls in alleviating particulate nitrate during a severe winter haze episode in northern China, Atmospheric Chemistry and Physics, 19, 5605-5613, 10.5194/acp-19-5605-2019, 2019.](#)
[Ye, Z., Guo, X., Cheng, L., Cheng, S., Chen, D., Wang, W., and Liu, B.: Reducing PM_{2.5} and secondary inorganic aerosols by agricultural ammonia emission mitigation within the Beijing-Tianjin-Hebei region, China, Atmospheric Environment, 219, 10.1016/j.atmosenv.2019.116989, 2019.](#)
[Cao, J.-J., Shen, Z.-X., Chow, J. C., Watson, J. G., Lee, S.-C., Tie, X.-X., Ho, K.-F., Wang, G.-H., and Han, Y.-M.: Winter and Summer PM_{2.5} Chemical Compositions in Fourteen Chinese Cities, Journal of the Air & Waste Management Association, 62, 1214-1226, 10.1080/10962247.2012.701193, 2012.](#)
[Huang, W., Cao, J., Tao, Y., Dai, L., Lu, S.-E., Hou, B., Wang, Z., and Zhu, T.: Seasonal Variation of Chemical Species Associated With Short-Term Mortality Effects of PM_{2.5} in Xi'an, a Central City in China, American Journal of Epidemiology, 175, 556-566, 10.1093/aje/kwr342, 2012.](#)
[Liu, Z., Gao, W., Yu, Y., Hu, B., Xin, J., Sun, Y., Wang, L., Wang, G., Bi, X., Zhang, G., Xu, H., Cong, Z., He, J., Xu, J., and Wang, Y.: Characteristics of PM_{2.5} mass concentrations and chemical species in urban and background areas of China: emerging results from the CARE-China network, Atmospheric Chemistry and Physics, 18, 8849-8871, 10.5194/acp-18-8849-2018, 2018.](#)
[Luo, Y., Zhou, X., Zhang, J., Xiao, Y., Wang, Z., Zhou, Y., and Wang, W.: PM_{2.5} pollution in a petrochemical industry city of northern China: Seasonal variation and source apportionment, Atmospheric Research, 212, 285-295, 10.1016/j.atmosres.2018.05.029, 2018.](#)
[Wang, H. L., Qiao, L. P., Lou, S. R., Zhou, M., Ding, A. J., Huang, H. Y., Chen, J. M., Wang, Q., Tao, S., Chen, C. H., Li, L., and Huang, C.: Chemical composition of PM_{2.5} and meteorological impact among three years in urban Shanghai, China, Journal of Cleaner Production, 112, 1302-1311, 10.1016/j.jclepro.2015.04.099, 2016a.](#)
[Wang, J., Li, X., Zhang, W., Jiang, N., Zhang, R., and Tang, X.: Secondary PM_{2.5} in Zhengzhou, China: Chemical Species Based on Three Years of Observations, Aerosol and Air Quality Research, 16, 91-104, 10.4209/aaqr.2015.01.0007, 2016b.](#)

Formatted: Line spacing: multiple 1.15 li

Wang, Q., Fang, J., Shi, W., and Dong, X.: Distribution characteristics and policy-related improvements of PM_{2.5} and its components in six Chinese cities, *Environmental Pollution*, 266, 10.1016/j.envpol.2020.115299, 2020.

Xu, Q., Wang, S., Jiang, J., Bhattarai, N., Li, X., Chang, X., Qiu, X., Zheng, M., Hua, Y., and Hao, J.: Nitrate dominates the chemical composition of PM_{2.5} during haze event in Beijing, China, *Science of the Total Environment*, 689, 1293-1303, 10.1016/j.scitotenv.2019.06.294, 2019.

Zhang, T., Cao, J. J., Tie, X. X., Shen, Z. X., Liu, S. X., Ding, H., Han, Y. M., Wang, G. H., Ho, K. F., Qiang, J., and Li, W. T.: Water-soluble ions in atmospheric aerosols measured in Xi'an, China: Seasonal variations and sources, *Atmospheric Research*, 102, 110-119, 10.1016/j.atmosres.2011.06.014, 2011.

Zheng, J., Hu, M., Peng, J., Wu, Z., Kumar, P., Li, M., Wang, Y., and Guo, S.: Spatial distributions and chemical properties of PM_{2.5} based on 21 field campaigns at 17 sites in China, *Chemosphere*, 159, 480-487, 10.1016/j.chemosphere.2016.06.032, 2016.

Chang, W., and Zhan, J.: The association of weather patterns with haze episodes: Recognition by PM_{2.5} oriented circulation classification applied in Xiamen, Southeastern China, *Atmospheric Research*, 197, 425-436, 10.1016/j.atmosres.2017.07.024, 2017.

Dai, H., Zhu, J., Liao, H., Li, J., Liang, M., Yang, Y., and Yue, X.: Co-occurrence of ozone and PM_{2.5} pollution in the Yangtze River Delta over 2013-2019: Spatiotemporal distribution and meteorological conditions, *Atmospheric Research*, 249, 10.1016/j.atmosres.2020.105363, 2021.

Ding, A., Huang, X., Nie, W., Chi, X., Xu, Z., Zheng, L., Xu, Z., Xie, Y., Qi, X., Shen, Y., Sun, P., Wang, J., Wang, L., Sun, J., Yang, X.-Q., Qin, W., Zhang, X., Cheng, W., Liu, W., Pan, L., and Fu, C.: Significant reduction of PM_{2.5} in eastern China due to regional-scale emission control: evidence from SORPES in 2011-2018, *Atmospheric Chemistry and Physics*, 19, 11791-11801, 10.5194/acp-19-11791-2019, 2019.

Fu, X., Wang, S., Xing, J., Zhang, X., Wang, T., and Hao, J.: Increasing Ammonia Concentrations Reduce the Effectiveness of Particle Pollution Control Achieved via SO₂ and NO_x Emissions Reduction in East China, *Environmental Science & Technology Letters*, 4, 221-227, 10.1021/acs.estlett.7b00143, 2017.

Xing, J., Ding, D., Wang, S., Zhao, B., Jang, C., Wu, W., Zhang, F., Zhu, Y., and Hao, J.: Quantification of the enhanced effectiveness of NO_x control from simultaneous reductions of VOC and NH₃ for reducing air pollution in the Beijing-Tianjin-Hebei

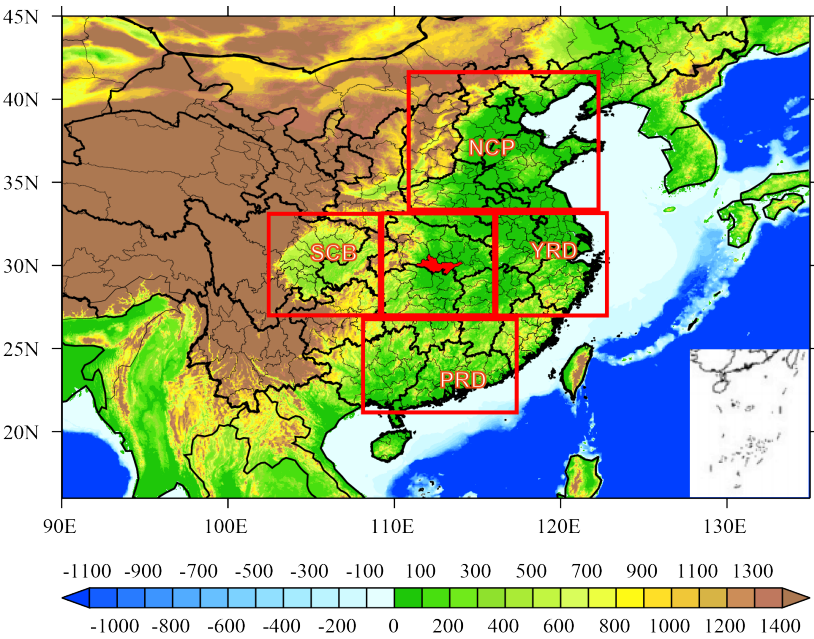
1655 [region, China, Atmospheric Chemistry and Physics, 18, 7799-7814, 10.5194/acp-18-](#)
1656 [7799-2018, 2018.](#)
1657 [Xing, J., Ding, D., Wang, S., Dong, Z., Kelly, J. T., Jang, C., Zhu, Y., and Hao, J.: Development and application of observable response indicators for design of an](#)
1658 [effective ozone and fine-particle pollution control strategy in China, Atmospheric](#)
1659 [Chemistry and Physics, 19, 13627-13646, 10.5194/acp-19-13627-2019, 2019.](#)
1660 [Philipp, A., Beck, C., Huth, R., and Jacobeit, J.: Development and comparison of](#)
1661 [circulation type classifications using the COST 733 dataset and software,](#)
1662 [International Journal of Climatology, 36, 2673-2691, 10.1002/joc.3920, 2016.](#)
1663 [Pope, R. J., Savage, N. H., Chipperfield, M. P., Arnold, S. R., and Osborn, T. J.: The](#)
1664 [influence of synoptic weather regimes on UK air quality: analysis of satellite column](#)
1665 [NO₂, Atmospheric Science Letters, 15, 211-217, 10.1002/asl2.492, 2014.](#)
1666 [Russo, A., Trigo, R. M., Martins, H., and Mendes, M. T.: NO₂, PM₁₀ and O₃ urban](#)
1667 [concentrations and its association with circulation weather types in Portugal,](#)
1668 [Atmospheric Environment, 89, 768-785, 10.1016/j.atmosenv.2014.02.010, 2014.](#)
1669 [Santurtun, A., Carlos Gonzalez-Hidalgo, J., Sanchez-Lorenzo, A., and Teresa](#)
1670 [Zarrabeitia, M.: Surface ozone concentration trends and its relationship with weather](#)
1671 [types in Spain \(2001-2010\), Atmospheric Environment, 101, 10-22,](#)
1672 [10.1016/j.atmosenv.2014.11.005, 2015.](#)
1673
1674 ▼

Formatted: Font:Font color: Auto

Formatted: EndNote Bibliography, Left, Indent: Left: 0 cm, Hanging: 1 ch, First line: -1 ch, Space Before: 0 pt, After: 0 pt, Don't add space between paragraphs of the same style, Line spacing: multiple 1.15 li, Widow/Orphan control, Adjust space between Latin and Asian text, Adjust space between Asian text and numbers

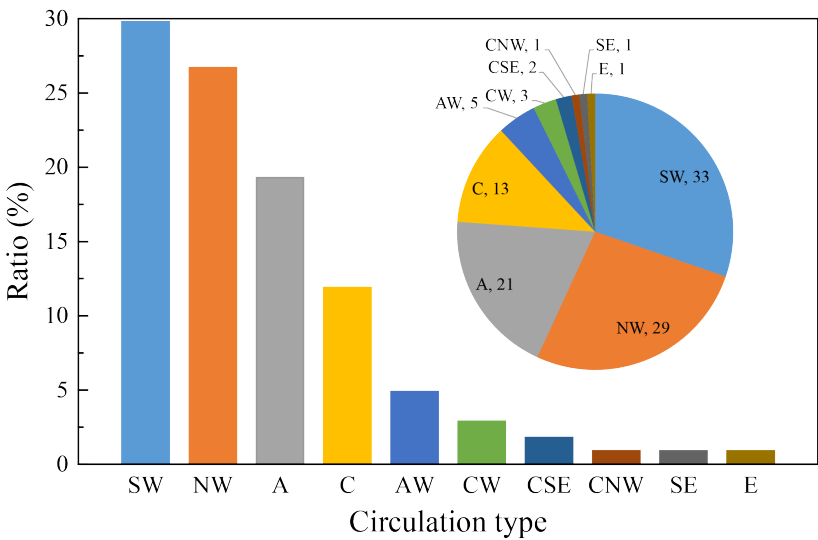
Deleted: .

1676
1677



1678
1679 Figure 1 The location of Jingzhou (red area) and the major haze pollution regions of
1680 NCP, YRD, PRD, and SCB. The areas framed in red are used to investigate the inter-
1681 regional imapcts by GEOS-Chem sensitivity simulations. The overlaid map shows the
1682 surface elevation (m) from a 2 min Gridded Global Relief Data (ETOPO2v2) available
1683 at NGDC Marine Trackline Geophysical database
1684 (<http://www.ngdc.noaa.gov/mgg/global/etopo2.html>).
1685

1686

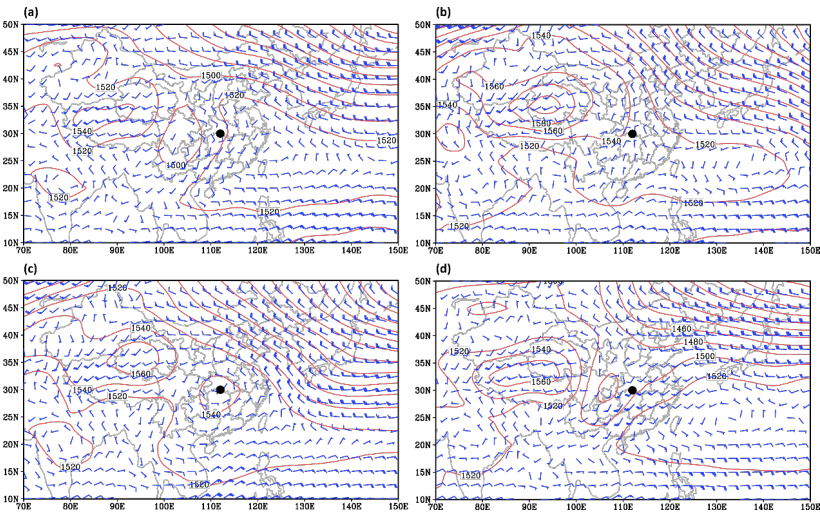


1687

1688 Figure 2 Frequency distributions of ten circulation types for the heavy pollution days
1689 of 2013-2018 over Jingzhou. The occurrence numbers of each type are shown. The ten
1690 circulation types include Southwest (SW), Northwest (NW), Anticyclone (A), Cyclone
1691 (C), Anticyclone-West (AW), Cyclone-West (CW), Cyclone-Southeast (CSE),
1692 Cyclone-Northwest (CNW), Southeast (SE) and East (E), respectively.

1693

1694



1695

1696

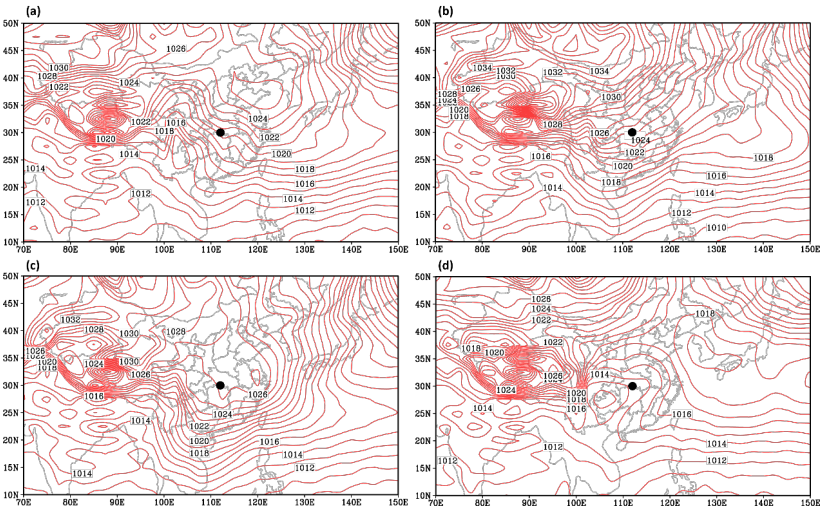
1697

1698

1699

Figure 3 Spatial distribution of 850 hPa geopotential height and wind vector for SW-type (a), NW-type (b), A-type (c) and C-type (d) synoptic control averaged over 2013-2018. The black dot indicates the location of Jingzhou.

1700



1701

1702

Figure 4 Spatial distribution of sea level pressure for SW-type (a), NW-type (b), A-type

1703

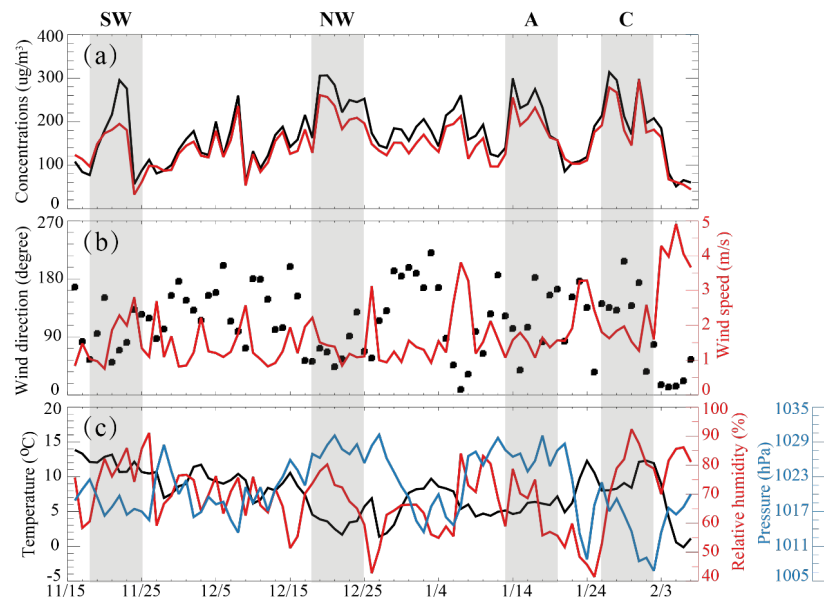
(c) and C-type (d) synoptic control averaged over 2013-2018. The black dot indicates

1704

the location of Jingzhou.

1705

1706



1708

1709 Figure 5 (a) Daily mean values of modeled (red line) and observed (black line) PM_{2.5}
1710 concentration (µg/m³) at Jingzhou and four severe pollution events (grey area) from
1711 November, 2013 to February, 2014. (b) Observed daily mean wind speed (red line) and
1712 wind direction (black dots). (c) Observed temperature (black line), relative humidity (red
1713 line) and sea level pressure (blue line).

1714

1715

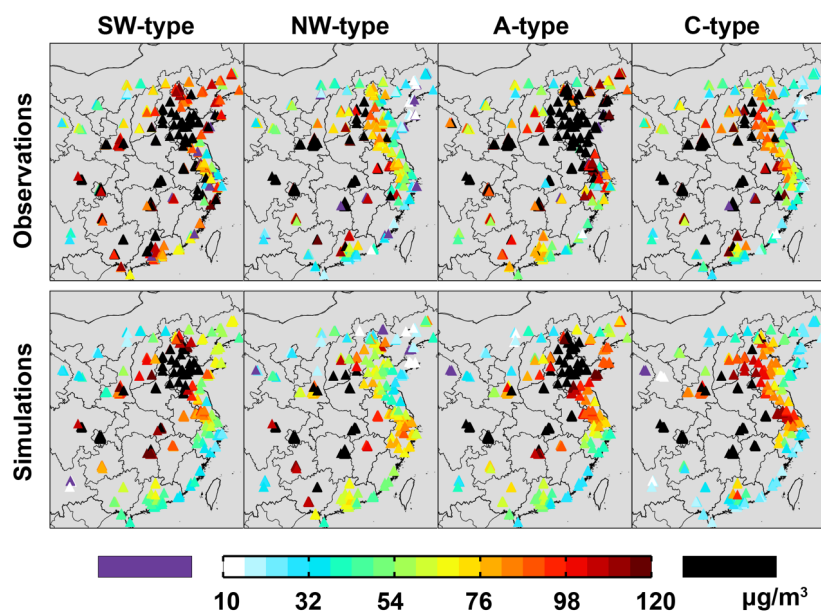
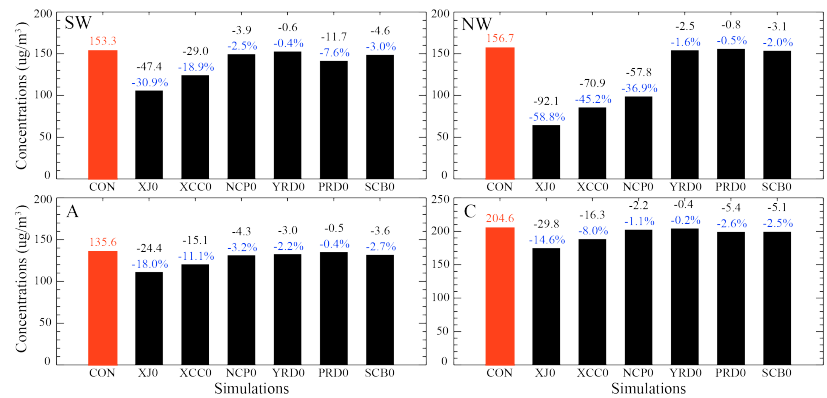


Figure 6 Spatial distribution of observed (top row) and modeled (bottom row, by CON case) PM_{2.5} concentrations (µg/m³) averaged over four severe pollution episodes controlled by SW-type (first column), NW-type (second column), A-type (third column) and C-type (forth column) synoptic pattern, respectively.

Formatted: Justified

1732



1733

1734

Figure 8. Modeled concentrations ($\mu\text{g}/\text{m}^3$) of $\text{PM}_{2.5}$ at Jingzhou in the GEOS-Chem control (red bar) and sensitivity (black bar) simulations in view of the regional transportation, and the differences (black characters for mass concentrations and blue characters for mass percentages) between the sensitivity and the control simulations. The abbreviations of each simulation referred to Table 2.

1739

1740

Deleted: 7

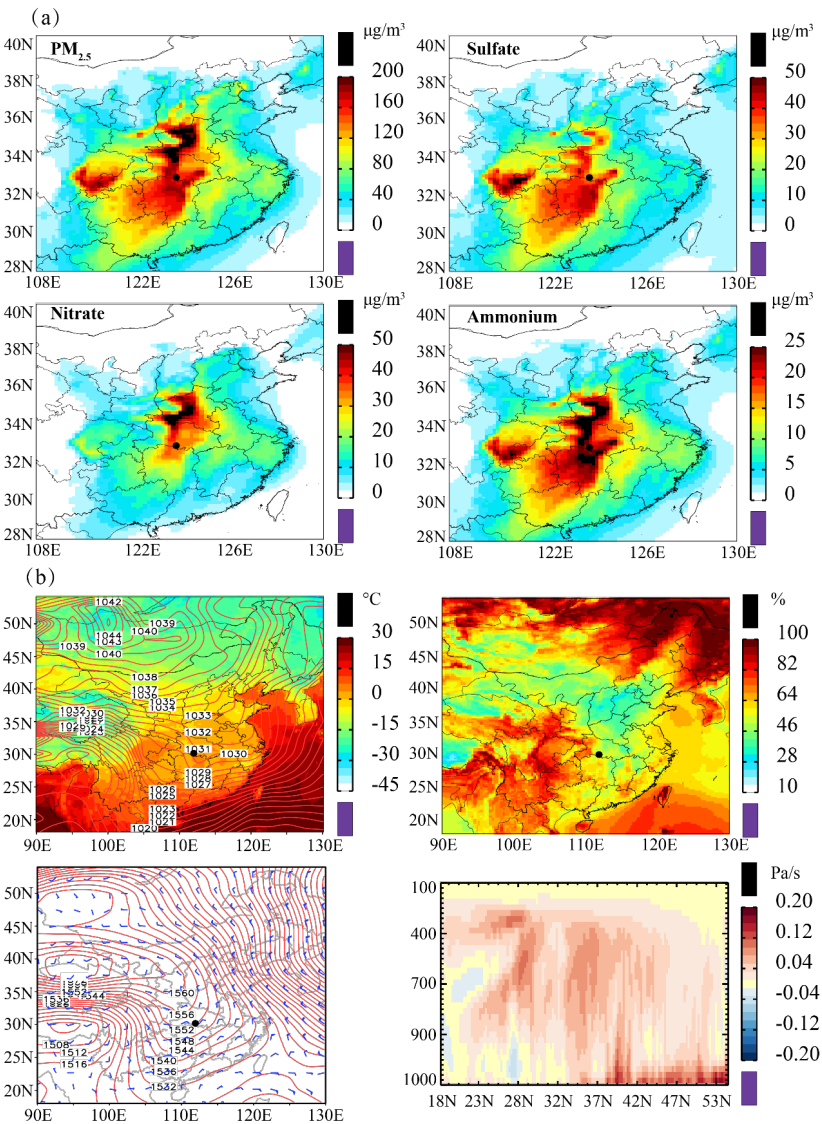


Figure 9. As in Fig. 6 but for NW-type synoptic control (19-26 December, 2013).

Deleted: 8

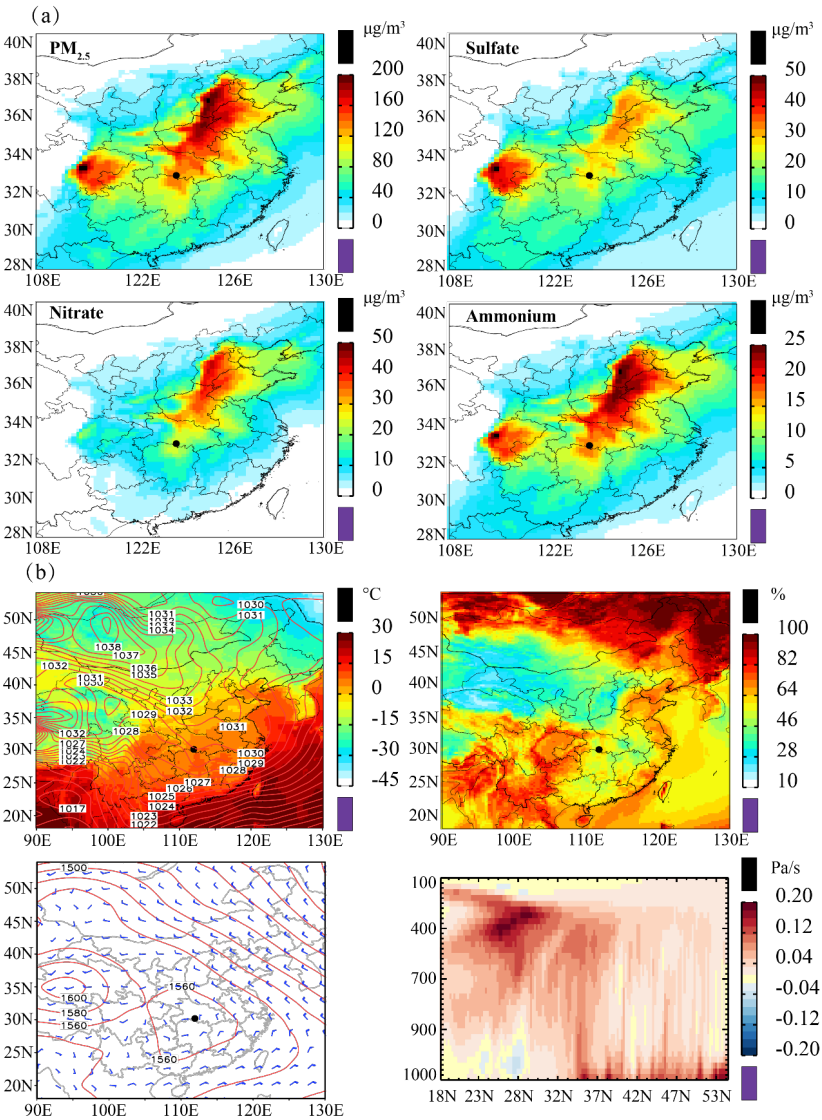


Figure 10. As in Fig. 6 but for A-type synoptic control (14-21 January, 2014).

Deleted: 9

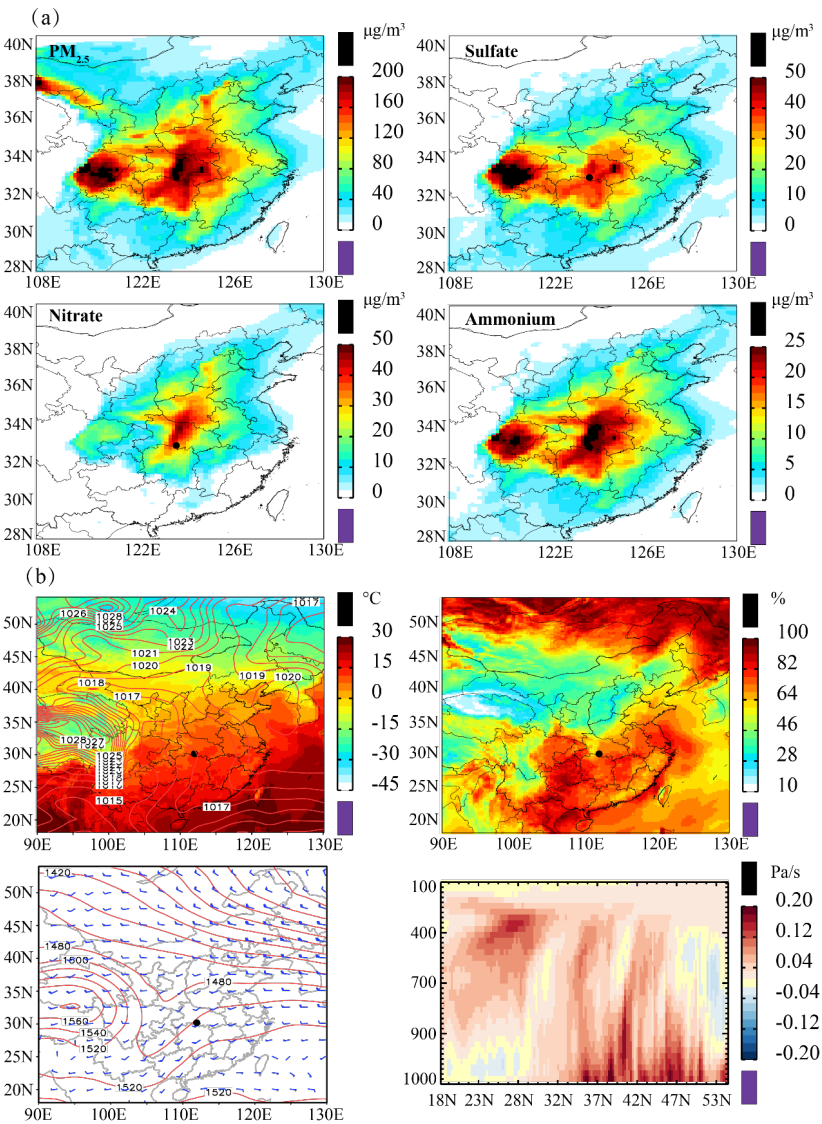
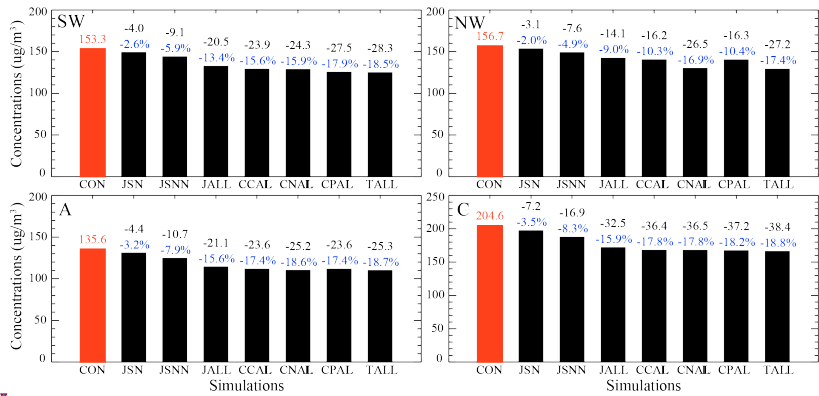


Figure 11. As in Fig. 6 but for C-type synoptic control (26 January - 2 February, 2014).

Deleted: 0

1760



1761

1762

1763

1764

1765

1766

1767

1768

Figure 12. Modeled concentrations ($\mu\text{g}/\text{m}^3$) of PM_{2.5} at Jingzhou in the GEOS-Chem control (red bar) and sensitivity (black bar) simulations for emission reduction, and the differences (black characters for mass concentrations and blue characters for mass percentages) between the sensitivity and the control simulations. The abbreviations of each simulation referred to Table 2.

Deleted:

Formatted: Font color: Black

Deleted: 1

1771
1772
|
1773
1774

Table 1 Lamb-Jenkinson circulation types

$ \xi \leq V$	$ \xi \geq 2V$	$V < \xi < 2V$
(Flat airflow type)	(Rotating airflow type)	(Mixed type)
East (E), Southeast (SE), Southwest (SW), Northwest (NW)	Anticyclone (A), Cyclone (C)	Cyclone-Southeast (CSE), Cyclone-West (CW), Cyclone-Northwest (CNW), Anticyclone-West (AW)

Formatted: Font:(Default) Times New Roman, 12 pt

1775

1776 Table 2 Description of sensitivity simulations by GEOS-Chem model. The NCP, YRD,

1777 PRD and SCB are the areas framed in red showed by Fig. 1.

Simulations	Description
CON	Applying the original emission situation in Table S1 and Table S2
XJ0	Emissions of all pollution sources ¹ outside Jingzhou are set to be zero
XCC0	Emissions of all pollution sources outside Central China are set to be zero
NCP0	Emissions of all pollution sources over NCP region are set to be zero
YRD0	Emissions of all pollution sources over YRD region are set to be zero
PRD0	Emissions of all pollution sources over PRD region are set to be zero
SCB0	Emissions of all pollution sources over SCB region are set to be zero
JSN	Emissions of SO ₂ and NO _x at Jingzhou are reduced by 20%
JSNN	Emissions of SO ₂ , NO _x and NH ₃ at Jingzhou are reduced by 20%
JALL	Emissions of all pollution sources at Jingzhou are reduced by 20%
CCALL	Emissions of all pollution sources over Central China are reduced by 20%
CNALL	Emissions of all pollution sources over Central China and NCP region are reduced by 20%
CPALL	Emissions of all pollution sources over Central China and PRD region are reduced by 20%
TALL	Emissions of all pollution sources over Central China, NCP, YRD, PRD and SCB region are reduced by 20%

1778

1. ¹ All pollution sources include emissions of SO₂, NO_x, NH₃, CO, BC, OC and NMVOCs.

1779

1780

1781

Formatted: Font:(Default) Times New Roman

1782

1783 Table 3 Simulated PM_{2.5} concentrations and associated chemical components averaged
1784 for the four typical heavy pollution episodes at Jingzhou. Also shown in brackets are
1785 the percentages of each component in PM_{2.5}.

PM _{2.5} components	Typical heavy pollution episodes			
µg/m ³	11/18-11/25 (SW-type)	12/19-12/26 (NW-type)	1/14-1/21 (A-type)	1/26-2/2 (C-type)
Nitrate	30.6 (20.0%)	34.6 (22.1%)	23.4 (17.3%)	42.3 (20.7%)
Sulfate	26.5 (13.4%)	30.7 (19.6%)	27.7 (20.4%)	40.4 (19.7%)
Ammonium	18.8 (12.3%)	21.6 (13.8%)	17.1 (12.6%)	27.1 (13.2%)
Dust	24.4 (15.9%)	22.3 (14.2%)	19.8 (14.6%)	29.2 (14.3%)
BC	10.5 (6.8%)	9.6 (6.1%)	9.5 (7.0%)	13.8 (6.7%)
POA	21.6 (14.1%)	18.9 (12.1%)	18.9 (13.9%)	27.7 (13.5%)
SOA	20.9 (13.6%)	19.0 (12.1%)	19.2 (14.2%)	24.1 (11.8%)
PM _{2.5}	153.3	156.7	135.6	204.6

1786

1787

1788 Table 4 The reported concentrations of PM_{2.5} and the three inorganic salts (sulfate,
1789 nitrate and ammonium, µg/m³) in other cities.

References	Site	Time	PM _{2.5}	Sulfate	Nitrate	Ammonium
Cao et al., 2012	Beijing	01/03	115.6±46.6	20.0±4.2 (17.3%)	13.1±4.5 (11.3%)	9.4±4.1 (8.1%)
Cao et al., 2012	Qingdao	01/03	134.8±43.0	21.1±7.7 (15.7%)	19.3±9.2 (14.3%)	15.3±5.2 (11.4%)
Cao et al., 2012	Tianjin	01/03	203.1±76.2	32.5±15.1 (16.0%)	25.2±10.3 (12.4%)	22.2±9.8 (10.9%)
Cao et al., 2012	Xi'an	01/03	356.3±118.4	53.8±25.6 (15.1%)	29.0±10.0 (8.1%)	29.8±11.5 (8.4%)
Cao et al., 2012	Chongqing	01/03	316.6±101.2	60.9±19.6 (19.2%)	18.1±6.4 (5.7%)	28.8±8.9 (9.1%)
Cao et al., 2012	Hangzhou	01/03	177.3±59.5	33.4±16.7 (18.8%)	25.7±14.8 (14.5%)	19.1±10.7 (10.8%)
Cao et al., 2012	Shanghai	01/03	139.4±50.6	21.6±12.3 (15.5%)	17.5±8.7 (12.6%)	14.5±5.9 (10.4%)
Cao et al., 2012	Wuhan	01/03	172.3±67.0	31.4±15.6 (18.2%)	22.2±10.7 (12.9%)	18.4±10.2 (10.7%)
Zhang et al., 2011	Xi'an	03/06-03/07	194.1	35.6 (18.3%)	16.4 (8.4%)	11.4 (5.9%)
Huang et al., 2012	Xi'an	01/06-02/06	235.8±125.1	44.8±31.3 (19.0%)	20.5±14.2 (8.7%)	14.5±10.8 (6.1%)
Wang et al., 2020	Jinan	10/17	104±54	14.4±9.2 (13.8%)	33.4±23.2 (32.1%)	13.0±8.3 (12.5%)
Wang et al., 2020	Shijiazhuang	10/17	152±109	19.3±19.6 (12.7%)	42.8±41.1 (28.2%)	18.2±17.1 (12.0%)
Wang et al., 2020	Wuhan	12/17	117±33	13.6±3.2	26.6±11.1	13.1±3.8

				(11.6%)	(22.7%)	(11.2%)	
Wang et al., 2016a	Zhengzhou	01/11-02/11	297±160	48±36	31±19	21±16	Formatted [64]
				(16.2%)	(10.4%)	(7.1%)	Formatted [65]
							Formatted [66]
							Formatted: Font color: Text 1
Wang et al., 2016a	Zhengzhou	01/12-02/12	234±125	23±10	22±9	16±5	Formatted [63]
				(9.8%)	(9.4%)	(6.8%)	Formatted [68]
							Formatted [69]
							Formatted [70]
							Formatted: Font color: Text 1
Wang et al., 2016a	Zhengzhou	01/13-02/13	337±168	56±39	39±20	31±18	Formatted [67]
				(16.6%)	(11.6%)	(9.2%)	Formatted [72]
							Formatted [73]
							Formatted [74]
							Formatted: Font color: Text 1
Luo et al., 2018	Zibo	12/06-02/07	224.9±85.4	40.1±19.2	18.1±9.0	21.7±10.2	Formatted [71]
				(17.9%)	(8.1%)	(9.7%)	Formatted [76]
							Formatted [77]
							Formatted [78]
							Formatted: Font color: Text 1
Wang et al., 2016b	Shanghai	12/11, 12/12, 12/13	73.9±57.5	12.2±9.2	14.6±12.2	8.2±6.7	Formatted [75]
				(16.5%)	(19.8%)	(11.1%)	Formatted [80]
							Formatted [81]
							Formatted [82]
							Formatted: Font color: Text 1
Xu et al., 2019	Beijing	02/17-03/17	180.5	20.1	45.6	22.5	Formatted [79]
				(11.1%)	(25.3%)	(12.5%)	Formatted: Font color: Text 1
							Formatted: Font color: Text 1
							Formatted: Font color: Text 1
Xu et al., 2019	Beijing	05/17-09/17	186.7	20.2	32.4	17.1	Formatted: Font color: Text 1
				(10.8%)	(17.4%)	(9.2%)	Formatted: Font color: Text 1
							Formatted: Font color: Text 1
							Formatted: Font color: Text 1
Xu et al., 2019	Beijing	10/17-11/17	167.5	17.9	44.5	20.9	Formatted: Font color: Text 1
				(10.7%)	(26.6%)	(12.5%)	Formatted: Font color: Text 1
							Formatted: Font color: Text 1
Zheng et al., 2016	Beijing	03/10-05/10	65.2±65.1	11.1±10.1	11.1±11.0	6.8±6.7	Formatted: Font color: Text 1
				(17.0%)	(17.0%)	(10.4%)	
Zheng et al., 2016	Beijing	07/09-08/09	88.9±39.1	23.0±13.9	16.2±11.8	11.8±6.8	Formatted: Font color: Text 1
				(25.9%)	(18.2%)	(13.3%)	
Zheng et al., 2016	Beijing	12/09-02/10	84.0±66.6	8.1±8.3	8.0±9.6	5.9±7.1	Formatted: Font color: Text 1
				(9.1%)	(9.0%)	(6.6%)	
Zheng et al., 2016	Guangzhou	11/10	73.3±16.5	16.6±4.0	5.7±3.8	6.2±2.0	Formatted: Font color: Text 1
				(22.6%)	(7.8%)	(8.5%)	
Zheng et al., 2016	Shenzhen	12/09	64.6±24.7	20.6±3.5	4.9±3.5	4.6±1.0	Formatted: Font color: Text 1
				(31.9%)	(7.6%)	(7.1%)	
Zheng et al., 2016	Wuxi	04/10-05/10	82.1±27.0	12.8±3.8	9.9±6.3	7.0±2.0	Formatted: Font color: Text 1

				(15.6%)	(12.1%)	(8.5%)	
Zheng et al., 2016	Jinhua	10/11-11/11	81.9±26.2	18.3±6.7	12.6±7.0	10.4±4.1	Formatted: Font color: Text 1
				(22.3%)	(15.4%)	(12.7%)	
Liu et al., 2018	Chongqing	2012-2013	73.5±30.5	19.7±9.6	6.5±6.2	6.1±2.7	Formatted: Font color: Text 1
				(26.8%)	(8.8%)	(8.3%)	
Liu et al., 2018	Shanghai	2012-2013	68.4±20.3	13.6±6.4	11.9±5.0	5.8±2.1	Formatted: Font color: Text 1
				(19.9%)	(17.4%)	(8.5%)	
Liu et al., 2018	Beijing	2012-2013	71.7±36.0	11.9±8.2	9.3±7.5	5.3±2.7	Formatted: Font color: Text 1
				(16.6%)	(13.0%)	(7.4%)	
1790							Formatted: Font color: Text 1

Page 77: [1] Formatted	Microsoft Office User	1/2/21 11:42 AM
Font color: Text 1		
Page 77: [2] Formatted	Microsoft Office User	1/3/21 12:42 PM
Font color: Text 1		
Page 77: [3] Formatted	Microsoft Office User	1/3/21 12:42 PM
Font color: Text 1		
Page 77: [3] Formatted	Microsoft Office User	1/3/21 12:42 PM
Font color: Text 1		
Page 77: [4] Formatted	Microsoft Office User	1/3/21 12:42 PM
Font color: Text 1		
Page 77: [4] Formatted	Microsoft Office User	1/3/21 12:42 PM
Font color: Text 1		
Page 77: [5] Formatted	Microsoft Office User	1/3/21 12:42 PM
Font color: Text 1		
Page 77: [5] Formatted	Microsoft Office User	1/3/21 12:42 PM
Font color: Text 1		
Page 77: [6] Formatted	Microsoft Office User	1/3/21 12:42 PM
Font color: Text 1		
Page 77: [6] Formatted	Microsoft Office User	1/3/21 12:42 PM
Font color: Text 1		
Page 77: [7] Formatted	Microsoft Office User	1/3/21 12:42 PM
Font color: Text 1		
Page 77: [8] Formatted	Microsoft Office User	1/3/21 12:42 PM
Font color: Text 1		
Page 77: [8] Formatted	Microsoft Office User	1/3/21 12:42 PM
Font color: Text 1		
Page 77: [9] Formatted	Microsoft Office User	1/3/21 12:42 PM
Font color: Text 1		
Page 77: [9] Formatted	Microsoft Office User	1/3/21 12:42 PM
Font color: Text 1		
Page 77: [10] Formatted	Microsoft Office User	1/3/21 12:42 PM
Font color: Text 1		
Page 77: [10] Formatted	Microsoft Office User	1/3/21 12:42 PM
Font color: Text 1		
Page 77: [11] Formatted	Microsoft Office User	1/3/21 12:42 PM
Font color: Text 1		
Page 77: [11] Formatted	Microsoft Office User	1/3/21 12:42 PM
Font color: Text 1		

Page 77: [12] Formatted	Microsoft Office User	1/3/21 12:42 PM
Font color: Text 1		
Page 77: [13] Formatted	Microsoft Office User	1/3/21 12:42 PM
Font color: Text 1		
Page 77: [13] Formatted	Microsoft Office User	1/3/21 12:42 PM
Font color: Text 1		
Page 77: [14] Formatted	Microsoft Office User	1/3/21 12:42 PM
Font color: Text 1		
Page 77: [14] Formatted	Microsoft Office User	1/3/21 12:42 PM
Font color: Text 1		
Page 77: [15] Formatted	Microsoft Office User	1/3/21 12:42 PM
Font color: Text 1		
Page 77: [15] Formatted	Microsoft Office User	1/3/21 12:42 PM
Font color: Text 1		
Page 77: [16] Formatted	Microsoft Office User	1/3/21 12:42 PM
Font color: Text 1		
Page 77: [16] Formatted	Microsoft Office User	1/3/21 12:42 PM
Font color: Text 1		
Page 77: [17] Formatted	Microsoft Office User	1/3/21 12:42 PM
Font color: Text 1		
Page 77: [18] Formatted	Microsoft Office User	1/3/21 12:42 PM
Font color: Text 1		
Page 77: [18] Formatted	Microsoft Office User	1/3/21 12:42 PM
Font color: Text 1		
Page 77: [19] Formatted	Microsoft Office User	1/3/21 12:42 PM
Font color: Text 1		
Page 77: [19] Formatted	Microsoft Office User	1/3/21 12:42 PM
Font color: Text 1		
Page 77: [20] Formatted	Microsoft Office User	1/3/21 12:42 PM
Font color: Text 1		
Page 77: [20] Formatted	Microsoft Office User	1/3/21 12:42 PM
Font color: Text 1		
Page 77: [21] Formatted	Microsoft Office User	1/3/21 12:42 PM
Font color: Text 1		
Page 77: [21] Formatted	Microsoft Office User	1/3/21 12:42 PM
Font color: Text 1		
Page 77: [22] Formatted	Microsoft Office User	1/3/21 12:42 PM

Font color: Text 1

Page 77: [23] Formatted	Microsoft Office User	1/3/21 12:42 PM
-------------------------	-----------------------	-----------------

Font color: Text 1

Page 77: [23] Formatted	Microsoft Office User	1/3/21 12:42 PM
-------------------------	-----------------------	-----------------

Font color: Text 1

Page 77: [24] Formatted	Microsoft Office User	1/3/21 12:42 PM
-------------------------	-----------------------	-----------------

Font color: Text 1

Page 77: [24] Formatted	Microsoft Office User	1/3/21 12:42 PM
-------------------------	-----------------------	-----------------

Font color: Text 1

Page 77: [25] Formatted	Microsoft Office User	1/3/21 12:42 PM
-------------------------	-----------------------	-----------------

Font color: Text 1

Page 77: [25] Formatted	Microsoft Office User	1/3/21 12:42 PM
-------------------------	-----------------------	-----------------

Font color: Text 1

Page 77: [26] Formatted	Microsoft Office User	1/3/21 12:42 PM
-------------------------	-----------------------	-----------------

Font color: Text 1

Page 77: [26] Formatted	Microsoft Office User	1/3/21 12:42 PM
-------------------------	-----------------------	-----------------

Font color: Text 1

Page 77: [27] Formatted	Microsoft Office User	1/3/21 12:42 PM
-------------------------	-----------------------	-----------------

Font color: Text 1

Page 77: [28] Formatted	Microsoft Office User	1/3/21 12:42 PM
-------------------------	-----------------------	-----------------

Font color: Text 1

Page 77: [28] Formatted	Microsoft Office User	1/3/21 12:42 PM
-------------------------	-----------------------	-----------------

Font color: Text 1

Page 77: [29] Formatted	Microsoft Office User	1/3/21 12:42 PM
-------------------------	-----------------------	-----------------

Font color: Text 1

Page 77: [29] Formatted	Microsoft Office User	1/3/21 12:42 PM
-------------------------	-----------------------	-----------------

Font color: Text 1

Page 77: [30] Formatted	Microsoft Office User	1/3/21 12:42 PM
-------------------------	-----------------------	-----------------

Font color: Text 1

Page 77: [30] Formatted	Microsoft Office User	1/3/21 12:42 PM
-------------------------	-----------------------	-----------------

Font color: Text 1

Page 77: [31] Formatted	Microsoft Office User	1/3/21 12:42 PM
-------------------------	-----------------------	-----------------

Font color: Text 1

Page 77: [31] Formatted	Microsoft Office User	1/3/21 12:42 PM
-------------------------	-----------------------	-----------------

Font color: Text 1

Page 77: [32] Formatted	Microsoft Office User	1/3/21 12:42 PM
-------------------------	-----------------------	-----------------

Font color: Text 1

Page 77: [33] Formatted	Microsoft Office User	1/3/21 12:42 PM
Font color: Text 1		
Page 77: [33] Formatted	Microsoft Office User	1/3/21 12:42 PM
Font color: Text 1		
Page 77: [34] Formatted	Microsoft Office User	1/3/21 12:42 PM
Font color: Text 1		
Page 77: [34] Formatted	Microsoft Office User	1/3/21 12:42 PM
Font color: Text 1		
Page 77: [35] Formatted	Microsoft Office User	1/3/21 12:42 PM
Font color: Text 1		
Page 77: [35] Formatted	Microsoft Office User	1/3/21 12:42 PM
Font color: Text 1		
Page 77: [36] Formatted	Microsoft Office User	1/3/21 12:42 PM
Font color: Text 1		
Page 77: [36] Formatted	Microsoft Office User	1/3/21 12:42 PM
Font color: Text 1		
Page 77: [37] Formatted	Microsoft Office User	1/3/21 12:42 PM
Font color: Text 1		
Page 77: [38] Formatted	Microsoft Office User	1/3/21 12:42 PM
Font color: Text 1		
Page 77: [38] Formatted	Microsoft Office User	1/3/21 12:42 PM
Font color: Text 1		
Page 77: [39] Formatted	Microsoft Office User	1/3/21 12:42 PM
Font color: Text 1		
Page 77: [39] Formatted	Microsoft Office User	1/3/21 12:42 PM
Font color: Text 1		
Page 77: [40] Formatted	Microsoft Office User	1/3/21 12:42 PM
Font color: Text 1		
Page 77: [40] Formatted	Microsoft Office User	1/3/21 12:42 PM
Font color: Text 1		
Page 77: [41] Formatted	Microsoft Office User	1/3/21 12:42 PM
Font color: Text 1		
Page 77: [41] Formatted	Microsoft Office User	1/3/21 12:42 PM
Font color: Text 1		
Page 77: [42] Formatted	Microsoft Office User	1/3/21 12:42 PM
Font color: Text 1		
Page 77: [43] Formatted	Microsoft Office User	1/3/21 12:42 PM
Font color: Text 1		

Page 77: [44] Formatted	Microsoft Office User	1/3/21 12:42 PM
Font color: Text 1		
Page 77: [44] Formatted	Microsoft Office User	1/3/21 12:42 PM
Font color: Text 1		
Page 77: [45] Formatted	Microsoft Office User	1/3/21 12:42 PM
Font color: Text 1		
Page 77: [45] Formatted	Microsoft Office User	1/3/21 12:42 PM
Font color: Text 1		
Page 77: [46] Formatted	Microsoft Office User	1/3/21 12:42 PM
Font color: Text 1		
Page 77: [46] Formatted	Microsoft Office User	1/3/21 12:42 PM
Font color: Text 1		
Page 77: [47] Formatted	Microsoft Office User	1/3/21 12:42 PM
Font color: Text 1		
Page 77: [47] Formatted	Microsoft Office User	1/3/21 12:42 PM
Font color: Text 1		
Page 77: [48] Formatted	Microsoft Office User	1/3/21 12:42 PM
Font color: Text 1		
Page 77: [49] Formatted	Microsoft Office User	1/3/21 12:42 PM
Font color: Text 1		
Page 77: [49] Formatted	Microsoft Office User	1/3/21 12:42 PM
Font color: Text 1		
Page 77: [50] Formatted	Microsoft Office User	1/3/21 12:42 PM
Font color: Text 1		
Page 77: [50] Formatted	Microsoft Office User	1/3/21 12:42 PM
Font color: Text 1		
Page 77: [51] Formatted	Microsoft Office User	1/3/21 12:42 PM
Font color: Text 1		
Page 77: [51] Formatted	Microsoft Office User	1/3/21 12:42 PM
Font color: Text 1		
Page 77: [52] Formatted	Microsoft Office User	1/3/21 12:42 PM
Font color: Text 1		
Page 77: [52] Formatted	Microsoft Office User	1/3/21 12:42 PM
Font color: Text 1		
Page 77: [53] Formatted	Microsoft Office User	1/3/21 12:42 PM
Font color: Text 1		
Page 77: [54] Formatted	Microsoft Office User	1/3/21 12:42 PM

Font color: Text 1

Page 77: [54] Formatted	Microsoft Office User	1/3/21 12:42 PM
-------------------------	-----------------------	-----------------

Font color: Text 1

Page 77: [55] Formatted	Microsoft Office User	1/3/21 12:42 PM
-------------------------	-----------------------	-----------------

Font color: Text 1

Page 77: [55] Formatted	Microsoft Office User	1/3/21 12:42 PM
-------------------------	-----------------------	-----------------

Font color: Text 1

Page 77: [56] Formatted	Microsoft Office User	1/3/21 12:42 PM
-------------------------	-----------------------	-----------------

Font color: Text 1

Page 77: [56] Formatted	Microsoft Office User	1/3/21 12:42 PM
-------------------------	-----------------------	-----------------

Font color: Text 1

Page 77: [57] Formatted	Microsoft Office User	1/3/21 12:42 PM
-------------------------	-----------------------	-----------------

Font color: Text 1

Page 77: [57] Formatted	Microsoft Office User	1/3/21 12:42 PM
-------------------------	-----------------------	-----------------

Font color: Text 1

Page 77: [58] Formatted	Microsoft Office User	1/3/21 12:42 PM
-------------------------	-----------------------	-----------------

Font color: Text 1

Page 77: [59] Formatted	Microsoft Office User	1/3/21 12:42 PM
-------------------------	-----------------------	-----------------

Font color: Text 1

Page 77: [59] Formatted	Microsoft Office User	1/3/21 12:42 PM
-------------------------	-----------------------	-----------------

Font color: Text 1

Page 77: [60] Formatted	Microsoft Office User	1/3/21 12:42 PM
-------------------------	-----------------------	-----------------

Font color: Text 1

Page 77: [60] Formatted	Microsoft Office User	1/3/21 12:42 PM
-------------------------	-----------------------	-----------------

Font color: Text 1

Page 77: [61] Formatted	Microsoft Office User	1/3/21 12:42 PM
-------------------------	-----------------------	-----------------

Font color: Text 1

Page 77: [61] Formatted	Microsoft Office User	1/3/21 12:42 PM
-------------------------	-----------------------	-----------------

Font color: Text 1

Page 77: [62] Formatted	Microsoft Office User	1/3/21 12:42 PM
-------------------------	-----------------------	-----------------

Font color: Text 1

Page 77: [62] Formatted	Microsoft Office User	1/3/21 12:42 PM
-------------------------	-----------------------	-----------------

Font color: Text 1

Page 78: [63] Formatted	Microsoft Office User	1/3/21 12:42 PM
-------------------------	-----------------------	-----------------

Font color: Text 1

Page 78: [63] Formatted	Microsoft Office User	1/3/21 12:42 PM
-------------------------	-----------------------	-----------------

Font color: Text 1

Page 78: [64] Formatted	Microsoft Office User	1/3/21 12:42 PM
Font color: Text 1		
Page 78: [64] Formatted	Microsoft Office User	1/3/21 12:42 PM
Font color: Text 1		
Page 78: [65] Formatted	Microsoft Office User	1/3/21 12:42 PM
Font color: Text 1		
Page 78: [65] Formatted	Microsoft Office User	1/3/21 12:42 PM
Font color: Text 1		
Page 78: [66] Formatted	Microsoft Office User	1/3/21 12:42 PM
Font color: Text 1		
Page 78: [66] Formatted	Microsoft Office User	1/3/21 12:42 PM
Font color: Text 1		
Page 78: [67] Formatted	Microsoft Office User	1/3/21 12:42 PM
Font color: Text 1		
Page 78: [67] Formatted	Microsoft Office User	1/3/21 12:42 PM
Font color: Text 1		
Page 78: [68] Formatted	Microsoft Office User	1/3/21 12:42 PM
Font color: Text 1		
Page 78: [68] Formatted	Microsoft Office User	1/3/21 12:42 PM
Font color: Text 1		
Page 78: [69] Formatted	Microsoft Office User	1/3/21 12:42 PM
Font color: Text 1		
Page 78: [69] Formatted	Microsoft Office User	1/3/21 12:42 PM
Font color: Text 1		
Page 78: [70] Formatted	Microsoft Office User	1/3/21 12:42 PM
Font color: Text 1		
Page 78: [70] Formatted	Microsoft Office User	1/3/21 12:42 PM
Font color: Text 1		
Page 78: [71] Formatted	Microsoft Office User	1/3/21 12:42 PM
Font color: Text 1		
Page 78: [71] Formatted	Microsoft Office User	1/3/21 12:42 PM
Font color: Text 1		
Page 78: [72] Formatted	Microsoft Office User	1/3/21 12:42 PM
Font color: Text 1		
Page 78: [72] Formatted	Microsoft Office User	1/3/21 12:42 PM
Font color: Text 1		
Page 78: [73] Formatted	Microsoft Office User	1/3/21 12:42 PM
Font color: Text 1		

Page 78: [73] Formatted	Microsoft Office User	1/3/21 12:42 PM
Font color: Text 1		
Page 78: [74] Formatted	Microsoft Office User	1/3/21 12:42 PM
Font color: Text 1		
Page 78: [74] Formatted	Microsoft Office User	1/3/21 12:42 PM
Font color: Text 1		
Page 78: [75] Formatted	Microsoft Office User	1/3/21 12:42 PM
Font color: Text 1		
Page 78: [75] Formatted	Microsoft Office User	1/3/21 12:42 PM
Font color: Text 1		
Page 78: [76] Formatted	Microsoft Office User	1/3/21 12:42 PM
Font color: Text 1		
Page 78: [76] Formatted	Microsoft Office User	1/3/21 12:42 PM
Font color: Text 1		
Page 78: [77] Formatted	Microsoft Office User	1/3/21 12:42 PM
Font color: Text 1		
Page 78: [77] Formatted	Microsoft Office User	1/3/21 12:42 PM
Font color: Text 1		
Page 78: [78] Formatted	Microsoft Office User	1/3/21 12:42 PM
Font color: Text 1		
Page 78: [78] Formatted	Microsoft Office User	1/3/21 12:42 PM
Font color: Text 1		
Page 78: [79] Formatted	Microsoft Office User	1/3/21 12:42 PM
Font color: Text 1		
Page 78: [79] Formatted	Microsoft Office User	1/3/21 12:42 PM
Font color: Text 1		
Page 78: [80] Formatted	Microsoft Office User	1/3/21 12:42 PM
Font color: Text 1		
Page 78: [80] Formatted	Microsoft Office User	1/3/21 12:42 PM
Font color: Text 1		
Page 78: [81] Formatted	Microsoft Office User	1/3/21 12:42 PM
Font color: Text 1		
Page 78: [81] Formatted	Microsoft Office User	1/3/21 12:42 PM
Font color: Text 1		
Page 78: [82] Formatted	Microsoft Office User	1/3/21 12:42 PM
Font color: Text 1		
Page 78: [82] Formatted	Microsoft Office User	1/3/21 12:42 PM

Font color: Text 1